REPORT DOCUMENTATION PAGE

READ INSTRUCTIONS BEFORE COMPLETING FORM

1. REPORT NUMBER: TR 6146

2. GOVT ACCESSION NO.

3. RECIPIENT'S CATALOG NUMBER

4. TITLE *(and Subtitle)*: OBSERVATIONS OF SEA SURFACE CONDITIONS DURING WEAP EXPERIMENT, MAY 1982: AN EXAMPLE OF REAL-TIME MONITORING OF THE UPPER OCEAN ENVIRONMENT

5. TYPE OF REPORT & PERIOD COVERED

6. PERFORMING ORG. REPORT NUMBER

7. AUTHOR(s): David H. Shonting, James J. Bisagni, and Daniel J. O'Neill

8. CONTRACT OR GRANT NUMBER(s)

9. PERFORMING ORGANIZATION NAME AND ADDRESS:
Naval Underwater Systems Center
Newport Laboratory
Newport, RI 02841

10. PROGRAM ELEMENT, PROJECT, TASK AREA & WORK UNIT NUMBERS

11. CONTROLLING OFFICE NAME AND ADDRESS:
Naval Underwater Systems Center
Newport Laboratory
Newport, RI 02841

12. REPORT DATE: 1 March 1984

13. NUMBER OF PAGES: 56

14. MONITORING AGENCY NAME & ADDRESS *(if different from Controlling Office)*

15. SECURITY CLASS. *(of this report)*: UNCLASSIFIED

15a. DECLASSIFICATION / DOWNGRADING SCHEDULE

16. DISTRIBUTION STATEMENT *(of this Report)*

Approved for public release; distribution unlimited.

17. DISTRIBUTION STATEMENT *(of the abstract entered in Block 20, if different from Report)*

18. SUPPLEMENTARY NOTES

19. KEY WORDS *(Continue on reverse side if necessary and identify by block number)*

Environmental Monitoring
Oceanography Experiments
Wave Measurements
WEAP Experiment
Current Measurements

20. ABSTRACT *(Continue on reverse side if necessary and identify by block number)*

Two environmental monitoring systems that provide information on the geometry, spectra, and directionality of surface waves were tested during an in-water experiment conducted by the Naval Underwater Systems Center. The experiment was carried out as part of the Weapons Environmental Acoustics Program (WEAP) off Block Island, RI, in May 1982. Preliminary results demonstrate the usefulness and reliability of the two systems in

DD FORM 1 JAN 73 1473

20. ABSTRACT (Cont'd)

remotely measuring sea surface conditions. Wave measurements and other environmental observations made during the experiment are presented, and application of the instrumentation to weapons testing is discussed.

NUSC Technical Report 6146
1 March 1984

Observations of Sea Surface Conditions During WEAP Experiment, May 1982: An Example of Real-Time Monitoring of the Upper Ocean Environment

David H. Shonting
James J. Bisagni
Weapon Systems Department

Daniel J. O'Neill
Vitro Laboratories

Naval Underwater Systems Center
Newport, Rhode Island / New London, Connecticut

PREFACE

This study was supported by the U.S. Coast Guard's Research and Development Office (Oil Spill Environment Studies) and the Naval Underwater Systems Center's Independent Research Program.

The technical reviewer for this report was P. R. Temple (Code 3633).

The assistance of CAPT Fred Pease and the crew of the R/V Shock of the University of Rhode Island's Department of Ocean Engineering for the buoy deployment and recovery operations is greatly appreciated. ENDECO Corporation of Marion, MA, provided use of the Tarbell computer system for data receiving/processing at the Block Island Field Station. Thanks are also owed to Mike Gordon of the University of Rhode Island (Kingston, RI) and Ray Garant of Southeastern Massachusetts University (Dartmouth, MA) for assistance in the field and in analysis of the data.

REVIEWED AND APPROVED: 1 March 1984

W. A. Von Winkle

W. A. Von Winkle
Associate Technical Director for Technology

TABLE OF CONTENTS

	Page
LIST OF ILLUSTRATIONS	ii
INTRODUCTION	1
THE WEAP EXPERIMENT: OBSERVATIONS OF SURFACE EFFECTS	3
INSTRUMENTATION AND DATA RECORDING	5
Type 956 Directional Wave-Track Buoy	5
Type 1015 Wave-Track/Current Meter Buoy	7
Mooring and Ground Tackle	9
Data Receiving, Recording, Storage, and Processing	9
PRELIMINARY RESULTS	14
Wind Data	14
Wave Observations	14
Current Data	29
EFFECTS OF BUOY MOTIONS ON CURRENT OBSERVATIONS	33
CONCLUSIONS	44
REFERENCES	46
APPENDIX A: DETAILS OF WAVE DATA PROCESSING	A-1
APPENDIX B: SAMPLES OF TARBELL ESTIMATES OF WAVE STATISTICS FOR VARIOUS WAVE CONDITIONS	B-1

LIST OF ILLUSTRATIONS

Figure		Page
1	Site of WEAP Experiment	4
2	ENDECO Type 956 Directional Wave-Track Buoy	6
3	Buoy Electronics	8
4	Frequency Response for Type 956 Wave-Track Buoy.	8
5	Geometric Representation of Directional Wave-Track Buoy Motion Showing Tilt Response to Orbital Shear	10
6	ENDECO 110 Current Meter with Electrical and Tethering Connections to the Wave-Track Buoy System	10
7	Arrangement of Ground Tackle and Mooring Lines for Buoy Systems	11
8	Arrangement of Buoy Systems/Data Receiving Stations Aboard USNS LYNCH and on Block Island	12
9	Wind Speed and Direction During WEAP Experiment.	15
10	Barometric Pressure During WEAP Experiment	16
11	Plot of Wave Data Made Aboard USNS LYNCH	17
12	Automatic Printout from Tarbell System at Block Island	18
13	Significant and Mean Wave Heights During WEAP Experiments	20
14	Variance of Vertical Displacement	21
15	Selected Auto Spectral Density Distributions from the Tarbell Computations	22
16	Wind and Wave Direction Vectors	24
17	Raw Data Plot for 18 May Record from the NUSC Wave Analysis Program Showing Current Direction/Speed and Wave Profiles During Low Wave Conditions	25
18	Spectrum for Wave Conditions Shown in Figure 17.	26
19	Raw Data Plot for 23 May Record Showing Relatively High Wave Conditions	27
20	Spectrum of Wave Data Shown in Figure 19	28
21	Sample of Current Speed and Direction Obtained on HP9825A Aboard USNS LYNCH	30
22	Current Speed and Direction for the WEAP Experiment	31
23	Lagrangian Hodographs of Current Data	32
24	Test Configuration for Tank Test of Current Meter	34
25	Positive Error in Current Measurement for Amplitudes of 40 and 63 cm and at Two Towing Speeds	36
26	Configuration of ENDECO Current Meter Attachment to Wave-Track Buoy Mooring Cable	38
27	Geometry of Displacement of Current Meter as the Mooring Line Oscillates Vertically	38
28	Model of the Free Surface Fluctuation and the Horizontal Current Response	40
29	Samples of Recorded Current Speed and Heave Displacement During Different Wave Conditions	41
30	Normalized Covariance Function Estimated for the Record Pairs Shown in Figure 29 for Ten 1-Second Lags	43

OBSERVATIONS OF SEA SURFACE CONDITIONS DURING WEAP EXPERIMENT, MAY 1982:

AN EXAMPLE OF REAL TIME-MONITORING OF THE UPPER OCEAN ENVIRONMENT

INTRODUCTION

A principal mission of the Naval Underwater Systems Center (NUSC) is to develop, test, and evaluate underwater weapon systems. This mission necessitates conducting field tests and experiments to evaluate system performance in the ocean environment. During at-sea testing operations, strong emphasis is placed upon deployment and exercising of the electronic, mechanical, and acoustic components of weapon systems, and often too little effort is made to adequately sample and define the ambient marine environment. This situation exists in spite of the well-known fact that extreme or highly variable oceanographic conditions can severely limit, alter, or disrupt the successful functioning of these complex weapon systems. Thus, when malfunctions or failures occur, the possible degrading effects of the ocean medium are often unrecorded and hence unknown. This situation is particularly undesirable since ocean field tests often require considerable expenditures of manpower and funds and, further, involve operations with surface ships and submarines whose available time is extremely limited.

The lack of proper environmental monitoring sometimes results from ignorance of what to measure. For the most part, however, there is only a limited capability to make those environmental measurements deemed important to support weapon tests and evaluations. This limitation does not result from the unavailability of the proper instrumentation since modern oceanographic instrumentation exists to measure and record a wide range of oceanic variables. Rather, the limitation results from the strong emphasis placed on testing and logistics in weapon field tests, especially those performed in conjunction with Navy vessels. This emphasis often imposes severe constraints on environmental monitoring, which, if done at all, usually is conducted on a "not-to-interfere basis."

As weapon systems become more sophisticated, there is a growing awareness that their successful operation becomes commensurately more related to environmental factors; these factors, then, must be better understood and better monitored. Environmental measurements in support of weapon tests are best afforded by rapid or synoptic sensor deployment and recovery prior to the actual tests, and/or real-time or quasi-real-time data monitoring and recording during the tests.

Submarines and their associated weapon systems operate primarily within the upper 100-200 meters of the ocean. It is in this upper layer, including the sea surface, that oceanographic conditions are most complex and difficult to predict. Specifically, the phenomena critical to practically all varieties of Navy operations are the sea surface effects produced by the wind, namely:

1. Surface waves, which create a rough and complex sea surface.

2. White caps and small-scale turbulence, which combine to diffuse air bubbles and turbulence downward from the surface.

3. Gross surface mixing by turbulent wave motions, which can alter the depth of the mixed layer and the intensity of the bounding thermocline.

These phenomena in turn produce detrimental effects upon acoustic systems and vehicles, specifically:

1. Dynamic wave motions and surface shear turbulence, which have disruptive effects on the dynamic stability of surface ships and near-surface submarines, as well as on the launching of submarine missiles as they pass through the sea-air interface.

2. Wind and turbulence-produced high frequency ambient noise, which interferes with or masks weapon acoustic functions.

3. Refraction, forward and backward scattering, and absorption, which cause signal loss of near-surface submarine sonar and in weapons frequency sound transmission.

The problem of trying to understand the effects of these surface phenomena on underwater systems is compounded because, of all conceivable oceanographic variables, surface wave and turbulence conditions are the most difficult to measure. It is with this realization that the Applied Oceanography Group of the NUSC Weapon Systems Department is embarking on a program to develop systems and techniques to better monitor and record much needed real-time information on wind-waves and associated surface phenomena critical to the operation of underwater weapon systems. The initial phase of this program involved testing and evaluating two specific environmental monitoring systems that provide information on the geometry, spectra, and directionality of surface waves and wind/wave-generated ambient noise.

The first of these systems is a directional wave-track buoy originally developed at the University of Rhode Island and produced by ENDECO Inc. of Marion, MA, as the Type 956 (reference 1). The second is a sea surface monitoring system developed by NUSC in conjunction with ENDECO Inc. under sponsorship of the U.S. Coast Guard. This system (ENDECO Type 1015) is a combination wave-track buoy and current meter intended for deployment in oil spill areas to provide on-scene real-time data for use by various operational personnel. Such monitoring is critical in making on-scene decisions about the deployment of equipment since high winds and wave conditions can render cleanup operations difficult or impossible.

An opportunity to test and utilize these two new environmental monitoring systems was afforded during the Weapons Environmental Acoustics Program (WEAP), an acoustic experiment conducted by NUSC near Block Island, RI, in May 1982. This report presents the results of the wave measurements and other environmental observations made in support of this experiment.

Moreover, it demonstrates how sea surface conditions can be monitored to provide, in real time, practical information needed for a variety of Navy and Coast Guard test and evaluation operations.

THE WEAP EXPERIMENT: OBSERVATIONS OF SURFACE EFFECTS

Project WEAP is an acoustic research study of the interaction of higher frequency sound with the sea surface, water volume, and the sea bottom. One objective of WEAP is to establish a data base using field measurements of forward and backward scattering from the sea surface and bottom together with propagation fluctuations and reverberation. The observations are to be made under a variety of oceanographic conditions. These data will assist in the development and verification of environmental acoustic models used to better understand and improve underwater weapons performance. Of particular interest are data from shallow water environments (depths less than 200 meters) where weapon systems appear to experience great difficulty, probably due to a combination of gross boundary effects together with the large temperature and salinity variations that commonly occur in coastal or continental shelf regions.

The WEAP experiment was performed 15-24 May 1982 on the inner continental shelf near Block Island, RI, using the USNS LYNCH on a multi-point moor; water depth was approximately 35 meters (figure 1). Acoustic measurements were made of both forward and backward scattering and reverberation over a wide range of surface wave conditions. The experiments were conducted using a bottom-mounted parametric projector and a four-hydrophone vertical array at about 300 meters separation (figure 1). Both systems were hard-wired to the LYNCH via 200-meter-long multiconductor sea cables, which permitted acoustic transmission and receiving to be controlled from the ship. The acoustic projector could be trained upward at various azimuths to register backscattering and reverberation and also could be aimed toward the receiver to obtain forward scattering and direct transmission measurements.

The interpretation of measurements of acoustic forward and backward scattering from the sea surface requires information on sea surface roughness, which is considered as the dominant factor. The wind-wave field contains a broad spectrum of wavelengths from a few millimeters to beyond a hundred meters. The type of interaction from sound rays impinging upon the wavy sea surface will depend upon the ratio of the acoustic wavelengths to those of the surface waves; a ratio much greater than unity produces simple specular reflection effects, whereas a very small ratio produces more complex scattering effects. The acoustic frequencies of interest for the WEAP experiment range from 10-30 kHz, the equivalent wavelengths being from 5-15 centimeters, which fall between those of the smaller wind wavelets (capillary waves) and the larger wind-driven gravity waves. Thus, with respect to the 10-30 kHz range, both specular and scattering effects could occur. Furthermore, wind speeds in excess of 6-7 meters/second produce white caps and bubble formation which, as has been stated, grossly increase surface scattering and attenuation, particularly at higher acoustic frequencies.

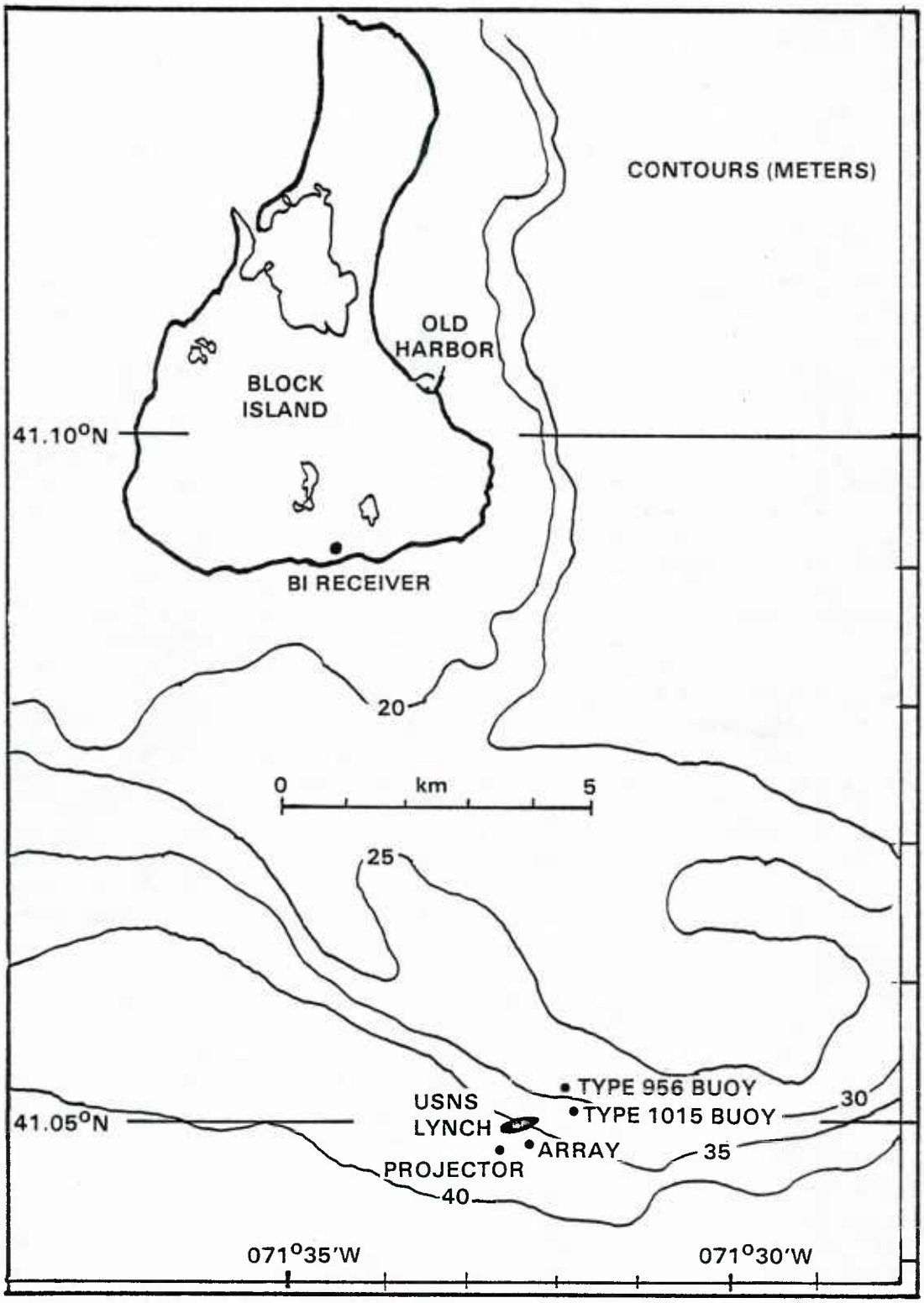

Figure 1. Site of WEAP Experiment

Acousticians have attempted to crudely model surface acoustic effects using parameters associated with the gross characteristics of the wind-wave field. Parameters variously described as associated with acoustic scattering at the sea surface are:

1. Sea surface slope or mean square slope (reference 2).

2. Auto spectra of the sea surface elevation (reference 3).

3. Mean peak-to-trough roughness or height (reference 4).

4. Air bubbles stirred into the upper few meters by high winds and white cap turbulence (reference 5).

Oceanographers do not at present have the capability to quantitatively measure the geometry of smaller waves and bubble size and concentrations, phenomena that directly affect acoustic waves; however, these phenomena are directly related to the existence of the larger dominant wind-waves which can now be measured. Further, it is clear that not only the sea surface roughness, but also its directivity can affect acoustic reflection and scattering in an azimuthal manner. Thus, by concentrating on the precise monitoring of the wind field and its associated surface waves, oceanographers can provide a background from which to begin to identify and examine the smaller scale phenomena so critical to acoustic propagation. Therefore, during the WEAP experiment the decision was made to monitor the free surface roughness, its directional characteristics, the occurrence of white caps, and wind speed and direction. A discussion of the environmental observations follows.

INSTRUMENTATION AND DATA RECORDING

The environmental observations were concerned with local wind waves (seas) and swell, current speed and direction, and meteorological data; all of these observations were made in the vicinity of the WEAP experiment conducted from the USNS LYNCH.

Surface waves were measured with two moored systems: a Type 956 directional wave-track buoy and a Type 1015 wave-track/current meter buoy, both manufactured by ENDECO, Marion, MA.

TYPE 956 DIRECTIONAL WAVE-TRACK BUOY

This system, originally developed by Middleton, LeBlanc, and Sternberger (reference 6) at the University of Rhode Island, and improved upon by ENDECO (reference 1), provides an FM telemetered record of both free surface displacement (or heave) and the gross directional characteristics of the wave field. The system (figure 2) utilizes an accelerometer to sense vertical heave as the buoy responds to the passing waves; the acceleration signal is doubly integrated to provide free surface displacement. The pitch and roll of the buoy, which together provide wave direction information, are detected by two tilt sensors that are coupled with a magnetic compass to provide

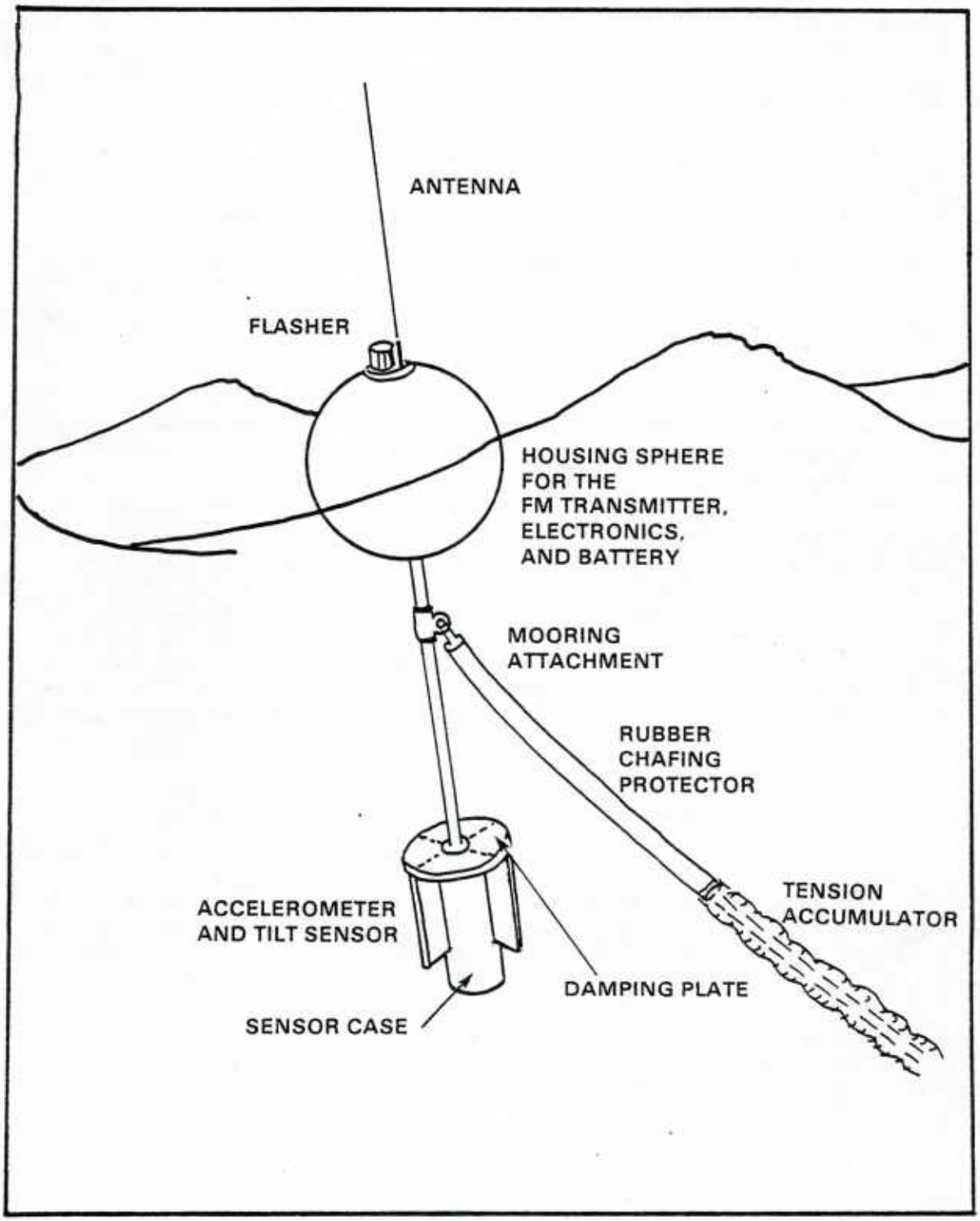

Figure 2. ENDECO Type 956 Directional Wave-Track Buoy

north-south and east-west tilting components as the axis of the buoy responds to the motions of the dominant wave trains.

Figure 3 shows a block diagram of the buoy electronics (taken from reference 1). The tilt sensors are differential capacitors orthogonally mounted in the horizontal plane to provide X and Y axis tilt recordings. A small reservoir of mercury on the inner wall of the housing causes change in the immersed capacitors as they oscillate with the buoy. The changes in capacity control an oscillator and demodulator circuit that supplies a ± 2 volt linear output over a range of $\pm 45^{\circ}$ tilt. The X and Y axis outputs are referenced to a two-axis flux gate compass to provide N-S and E-W heading information. The accelerometer is doubly integrated to provide free surface displacement. This output is then combined with the compass-referenced tilt output to drive voltage-controlled sine wave oscillators with IRIG (interrange instrumentation group) bands using center frequencies of 2300, 1300, and 730 Hz. Data are telemetered using an FM transmitter link of 100 mW with a nominal 40 MHz carrier. The pitch, roll, compass, and accelerometer instrumentation is housed in the bottom pressure case, and the transmitter electronics and battery pack are located in the spherical surface buoy (figure 2).

The basic motions of the buoy are: (1) vertical heave due to changing buoyant force on the sphere float as the sea surface level changes from passing waves, and (2) oscillatory tilting of the wave buoy axis from vertical due to horizontal shear forces associated with the wave orbital motions.

The heave response of the buoy system to surface waves (figure 4) displays a plateau from 0.035 - 4.0 Hz (i.e., periods from 2.5 - 30 seconds). This encompasses all but the smallest wind-waves and all swell frequencies.

The buoy system is moored at the center of horizontal drag, a predetermined point on the stainless-steel shaft connecting the sphere and the submerged instrument package (figure 2), which acts as a fulcrum of the inverted pendulum. This geometry allows the buoy to move in phase with the dominant orbital motions of the surface waves (figure 5). The buoy responds to the surface velocity shear associated with the orbital motions in such a manner that it experiences maximum tilt at the crest and trough of the waves. Since the motion of the buoy is in phase with the orbital motions, its natural period of pitching in effect filters out higher frequency wave motions; this in-phase condition also minimizes traumatic or irregular perturbations on the buoy's motion by breaking wave crests. A horizontal damping plate at the top of the sensor case (figure 2) provides a 0.6 critical damping of the buoy on the heave axis.

TYPE 1015 WAVE-TRACK/CURRENT METER BUOY

This system is identical to the 956 directional wave-track buoy except that it is coupled to a near-surface recording current meter (Type 110, manufactured by ENDECO). The current meter provides two channels, speed and direction, which are substituted for the two channels of NS and EW tilt information provided by the 956 system. The 1015 system thus provides real-time telemetered signals of free surface displacement along with current speed and direction. The heave response of the 1015 system to surface waves, however, is identical to that of the 956 system.

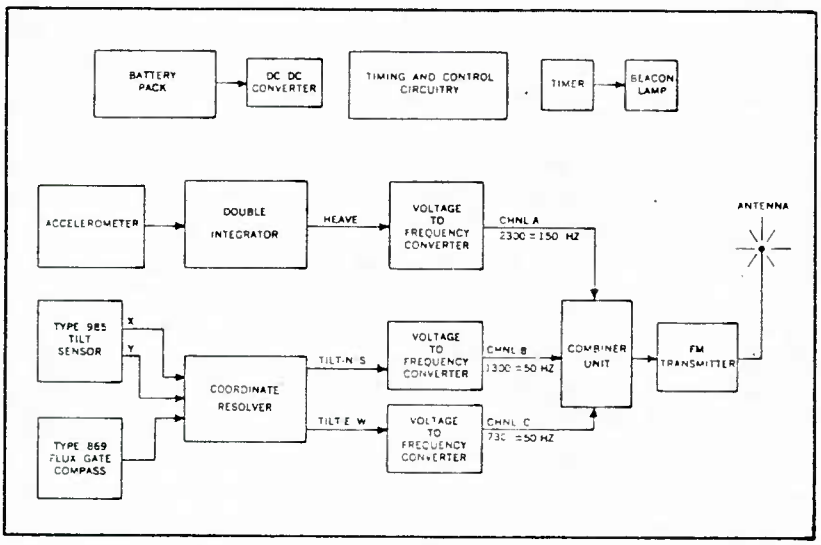

Figure 3. Buoy Electronics

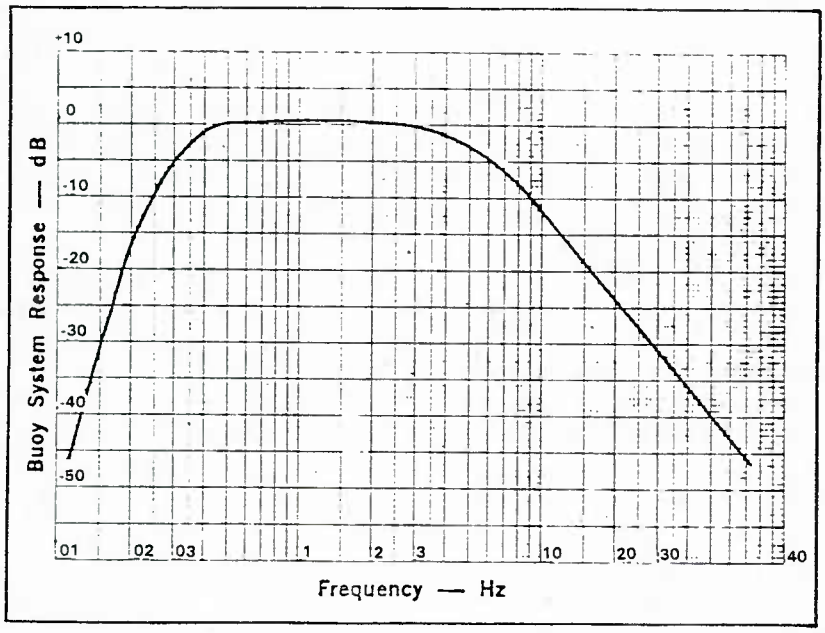

Figure 4. Frequency Response for Type 956 Wave-Track Buoy

The ENDECO 110 current meter (figure 6) is tethered to the mooring line 5 meters below a modified 956 directional wave-track buoy via a 1.6-meter-long nylon line that allows the mooring line to rise and fall with the surface wave motions while minimizing the perturbations on the current meter. For wave heights above 2-3 meters, however, oscillations in the current speed output can occur due to the surge on the tether line; these oscillations may require lowpass filtering below about 0.1 Hz. (Further discussion of possible effects of wave motions on the current data will be given under the heading "Effects of Buoy Motions on Current Observations."

MOORING AND GROUND TACKLE

The 956 and 1015 wave-track buoys each utilize a simple lightweight slack mooring that minimizes problems of deployment and retrieval (figure 7). The mooring line connecting to the buoy shaft is protected from chafing by a rubber hose (figure 2). Below the mooring line is a rubber accumulator that provides compliant response from 0-90 kilograms by a rubber cord that can be elongated up to 300 percent. A loosely woven nylon overbraid takes up the strain when the rubber is stretched beyond 300 percent. A nylon laid line, 16 millimeters in diameter with a 2.5-3.0 scope, leads to conventional chain and Danforth anchor ground tackle equipment. (The scope is the ratio of line length to water depth.) The relatively light ground tackle allows for deployment and recovery from a small boat, yet provides maximum holding with sufficient chain and scope.

DATA RECEIVING, RECORDING, STORAGE, AND PROCESSING

The arrangement of the data receiving stations for the WEAP experiment is shown in figure 8. The FM transmission from the directional wave-track buoy was made for a 20-minute period commencing each odd hour; for the wave-track/current meter buoy the 20-minute transmission began at even hours.

The telemetered data from the 956 and 1015 systems were collected by two Type 956 receiver processors (manufactured by ENDECO). One receiver processor, which was located aboard the USNS LYNCH, collected data via a UHF omnidirectional antenna mounted near the bridge; the other receiver processor, located on a cliff at the Block Island Field Station at Monhegan Bluffs, collected data some 40 meters above sea level via a UHF directional antenna manufactured by Cushcraft, Manchester, NH.

Each receiver filters the combined heave and directional tilt channels using IRIG bandpass filters. Phase lock loop demodulators provide additional noise rejection and dc signal analogs of the heave and two tilt channels. From the multiplexer output an A/D converter digitizes the analog signals into 8-bit binary code. A universal asynchronous receiver transmitter converts the three-channel parallel data into several outputs via an RS-232-C (serial digital interface connection) to provide for data transmission processing and storage.

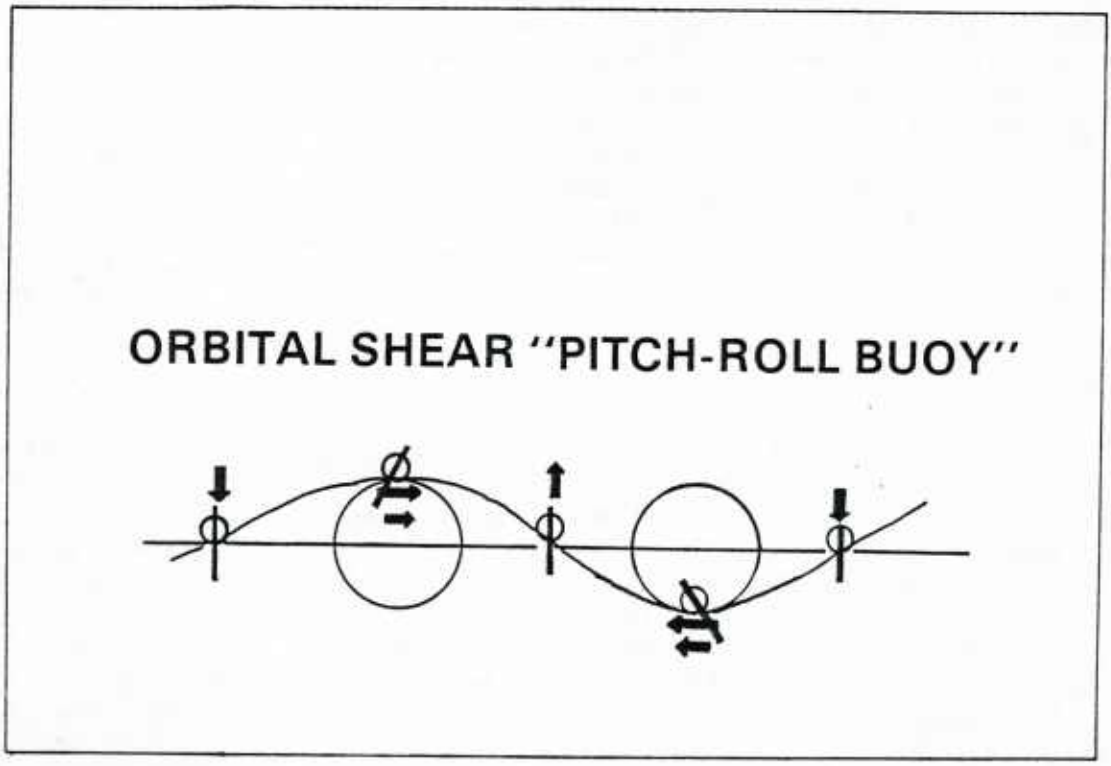

Figure 5. Geometric Representation of Directional Wave-Track Buoy Motion Showing Tilt Response to Orbital Shear

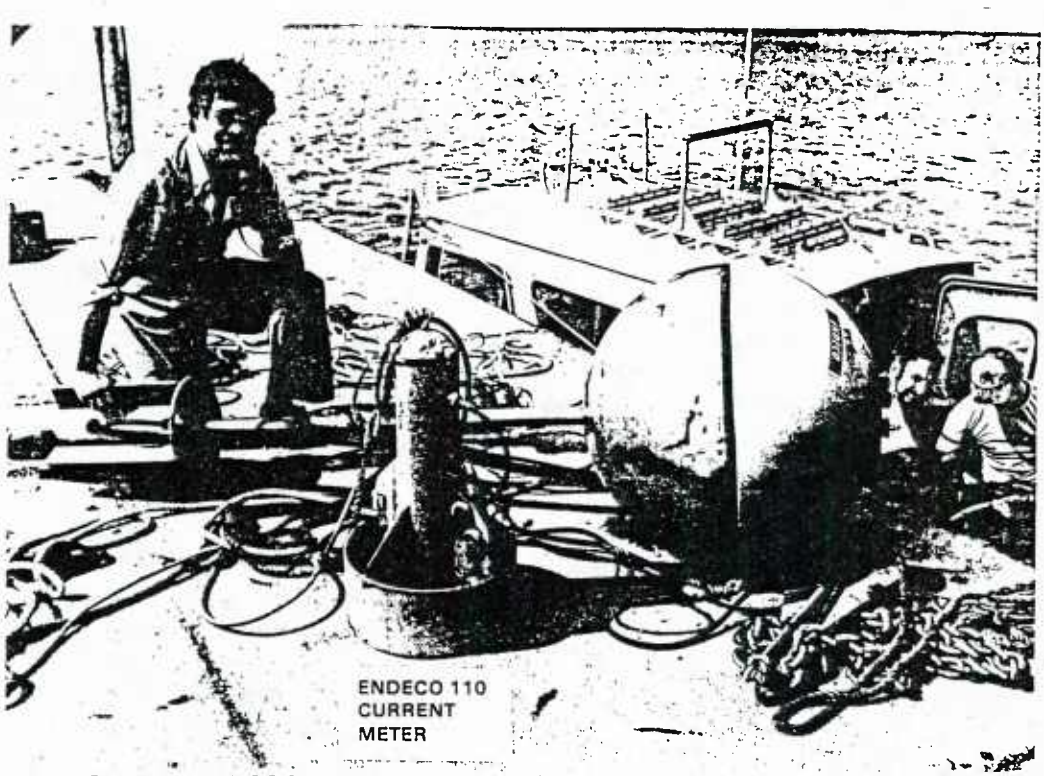

Figure 6. ENDECO 110 Current Meter System with Electrical and Tethering Connections to the Wave-Track Buoy System

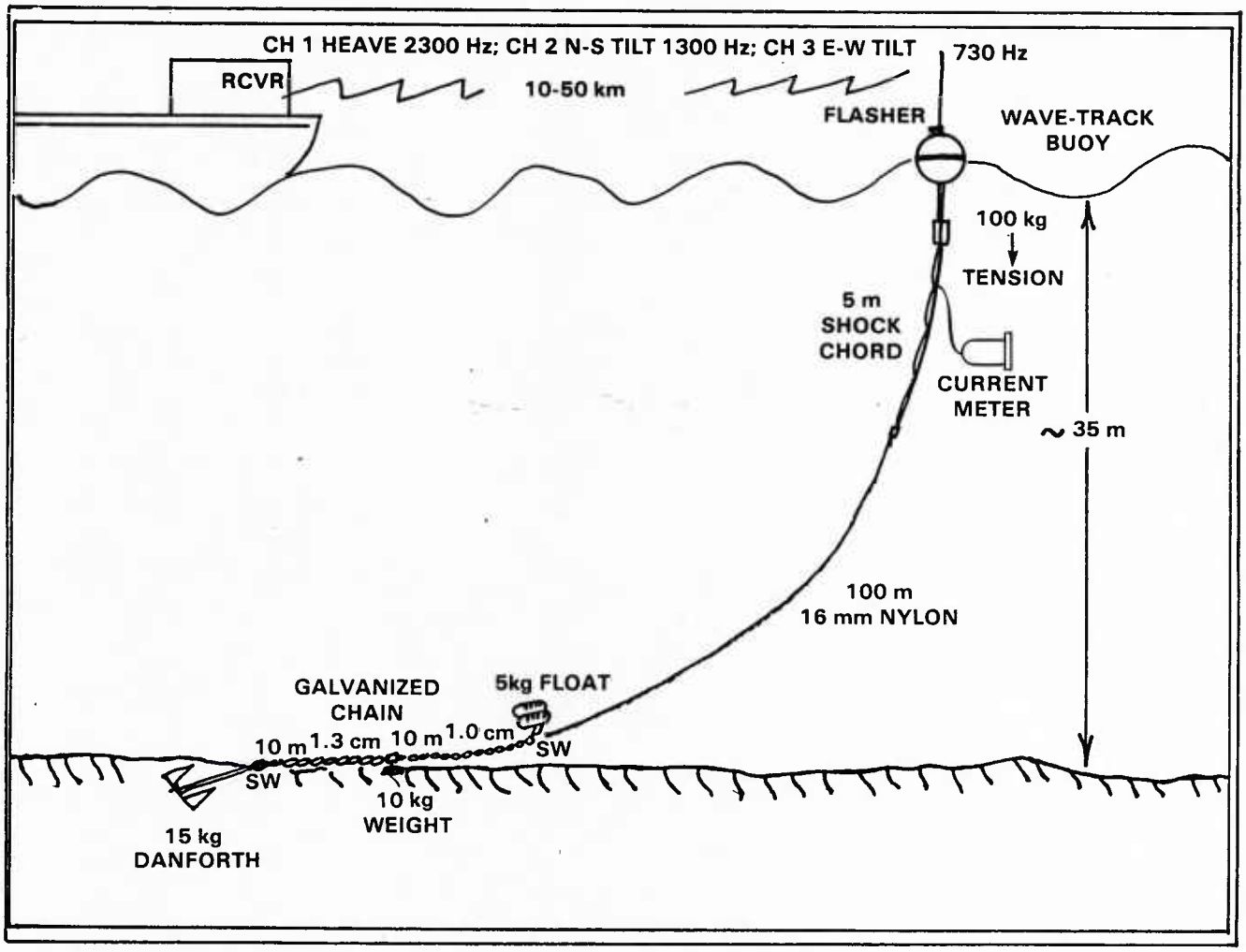

Figure 7. Arrangement of Ground Tackle and Mooring Lines Used for Buoy Systems

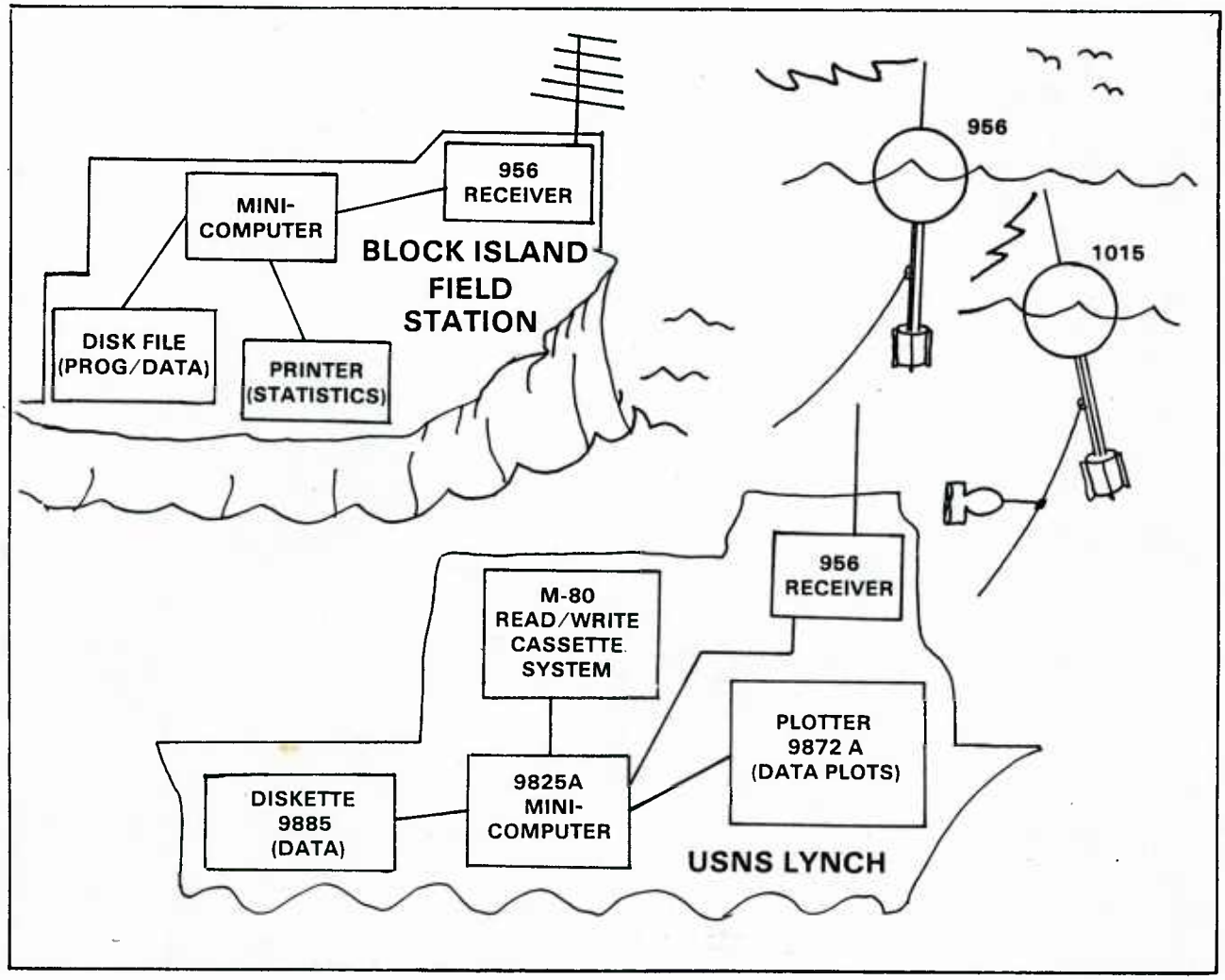

Figure 8. Arrangement of Buoy Systems/Data Receiving Stations Aboard the USNS LYNCH and on Block Island

The general sequence of telemetered wave buoy data collected aboard the LYNCH began with reception by an ENDECO 956 receiver that relayed digitized signals to a Memodyne M-80 cassette recorder for primary storage. (This machine is manufactured by Memodyne, Needham Heights, MA.) A single cassette could store all data gathered over 24 hours. Intermittently, data were transferred from the M-80 cassettes to diskettes using an HP9825A computer (manufactured by Hewlett-Packard, Loveland, CO). Subsequent analyses, consisting of data verification and time-series plot construction, accessed the disk data sets using an HP9825A computer. This freed the M-80 recorder for further immediate storage of new data. (Details of the procedures for processing the telemetered data aboard the LYNCH are given in appendix A.)

The telemetered data received at the Block Island Field Station were delivered through the RS-232-C output of the 956 receiver processor and read by a Tarbell minicomputer (manufactured by TIE, San Jose, CA). Processed data and statistical results were written on floppy disks in a Morrow design disk drive and presented each hour on an electronic printer.

The processing and analyses are performed by the Tarbell minicomputer as follows: From the diskette the program reads the data file, which contains time series of heave, NS tilt, and EW tilt, and performs a Fast Fourier Transform (FFT) on each time series. The range of frequencies is divided into 10 bands bordered on the upper end by the Nyquist frequency of 0.5 Hz (for a 1-second sampling rate). For each frequency band a digital bandpass filter is applied and corrections in amplitude and phase, determined from the wave buoy heave response calibration, are made. Auto spectra are calculated on the heave data, and an inverse FFT is performed on the data to produce filtered time series records.

The heave record is then subjected to a zero upcrossing analysis whereby individual waves are defined by consecutive upcrossings through the zero reading (defined as the mean value of the record). This enables estimates to be made of the following quantities:

1. Number of waves.
2. Maximum period.
3. Mean period.
4. Mean height.
5. Maximum height.
6. Period of maximum height.
7. Significant period (mean of the highest one-third of all periods).
8. Significant height (mean of the highest one-third of all waves).
9. Height variance.
10. Root-mean-square height.
11. The profile height of the maximum height wave at 1.0-second intervals.

Finally, the buoy tilt at each wave crest is computed from the tilt component data, and the mean wave direction and standard deviation are estimated for each of the 10 frequency band intervals. The entire statistical set plus comments on the data quantity and quality were printed out each hour. (Details of the computer program provided for the wave data analysis are given in reference 7.)

In addition, statistical and spectra analyses were done at the NUSC Newport laboratory on the wave data obtained aboard the USNS Lynch. The spectra were generated using the standard Fast Fourier Transform techniques discussed in reference 8. The NUSC analyses program, using the HP9825 A computer, produced the raw data plots and the auto spectra together with pertinent sampling parameters, environmental data, and statistical parameters. Discussion of the NUSC auto spectra is given in the next section.

PRELIMINARY RESULTS

WIND DATA

Wind speed and direction were measured hourly from the USNS LYNCH while on anchor station for the acoustic tests from 17 May 1982 until sea conditions forced the LYNCH to leave the mooring area on 23 May 1982. In addition, meteorological records were obtained from nearby U.S. Coast Guard stations at the Southeast Light House, Block Island, RI (an automated monitor having frequent data dropout), Point Judith, RI, and Montauk Point, NY.

The wind direction and speed (figure 9) displayed a variety of conditions that included two periods of moderately high winds reaching 10-11 meters/second from S, SW on 19-20 May followed by a weak "Northeaster" on 22-23 May accompanied by rain. Hatched areas in figure 9 designate periods when winds exceeded 7 meters/second at which white capping normally occurs. The barometric pressure (figure 10) indicates a weak low pressure moving through the area during 19-21 May, which was associated with the unsettled conditions accompanied by E, NE winds and showers.

WAVE OBSERVATIONS

The wave records in the form of free surface elevation and XY tilt measured on the ENDECO 956 system and the free surface elevation measured on the ENDECO 1015 system were recorded at both the LYNCH and Block Island receivers. The 956 and 1015 systems were located at the positions shown in figure 1.

A typical plot of the ENDECO 956 record processed on the HP9825A computer aboard the LYNCH is shown in figure 11. The mean sea surface is not quite centered precisely at 0 meters and appears to decrease with time, both effects being due to a slight dc drift in the voltage analog circuit. (This has minimal effect upon the statistics of the fluctuations except for a slight bias in the variance estimate.)

At Block Island the Tarbell computer/printer system generated a complete statistical summary (discussed in section 3) following each hourly data transmission. Figure 12 shows the printout for the Type 956 directional wave-track buoy. The insert shows a piece of the Rustrak monitor trace for the free surface record. Unfortunately the Tarbell program incorporates units in feet instead of meters.

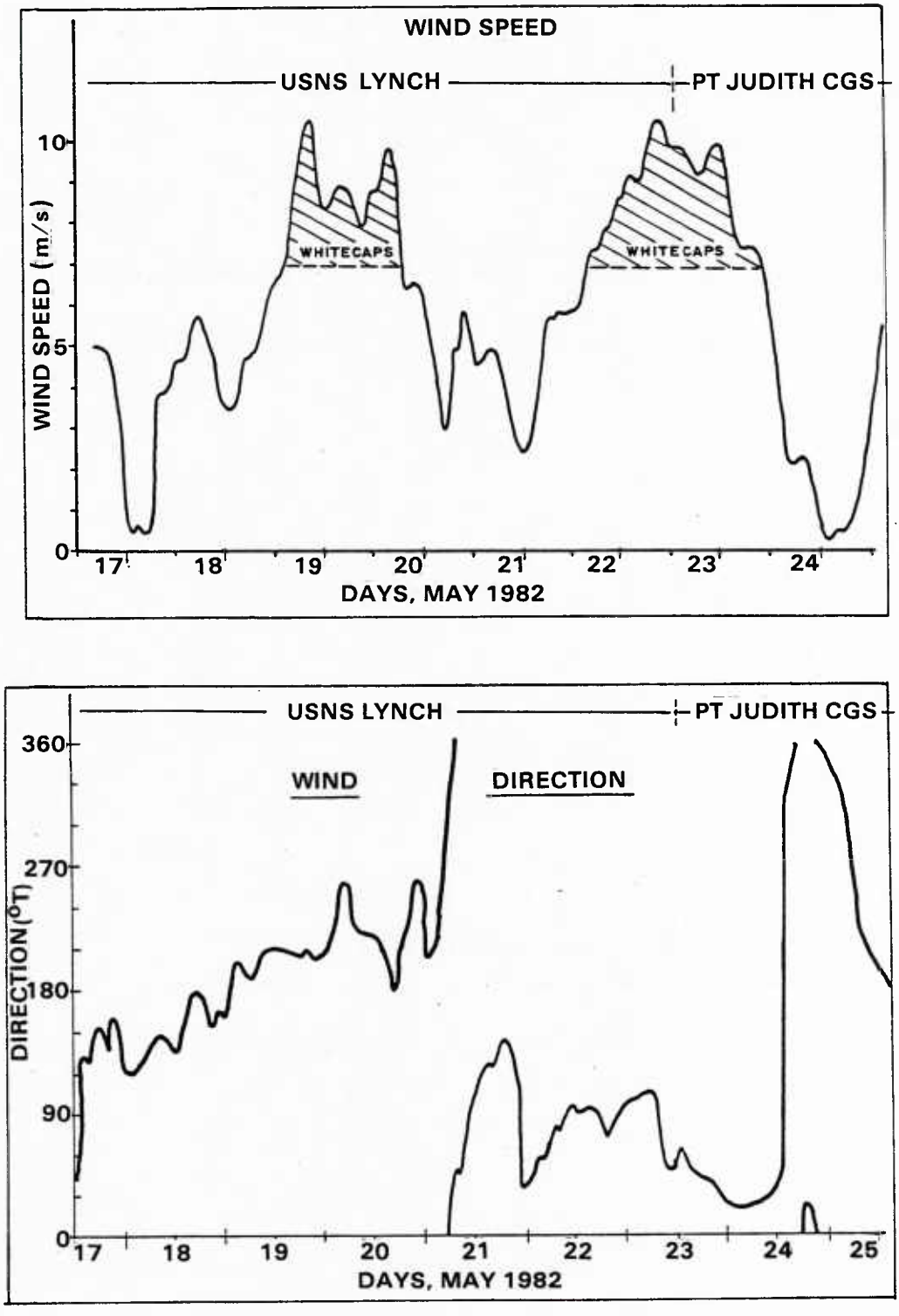

Figure 9. Wind Speed and Direction During the WEAP Experiment

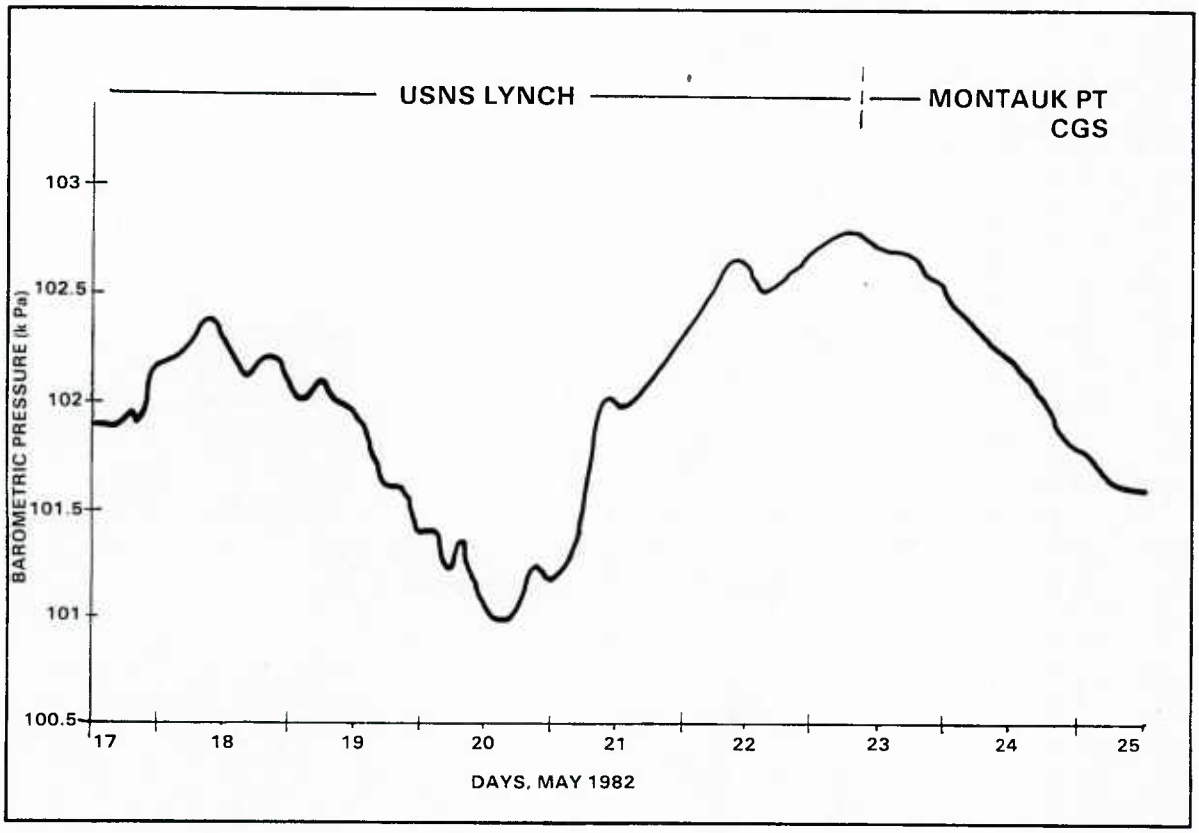

Figure 10. Barometric Pressure During WEAP Experiment

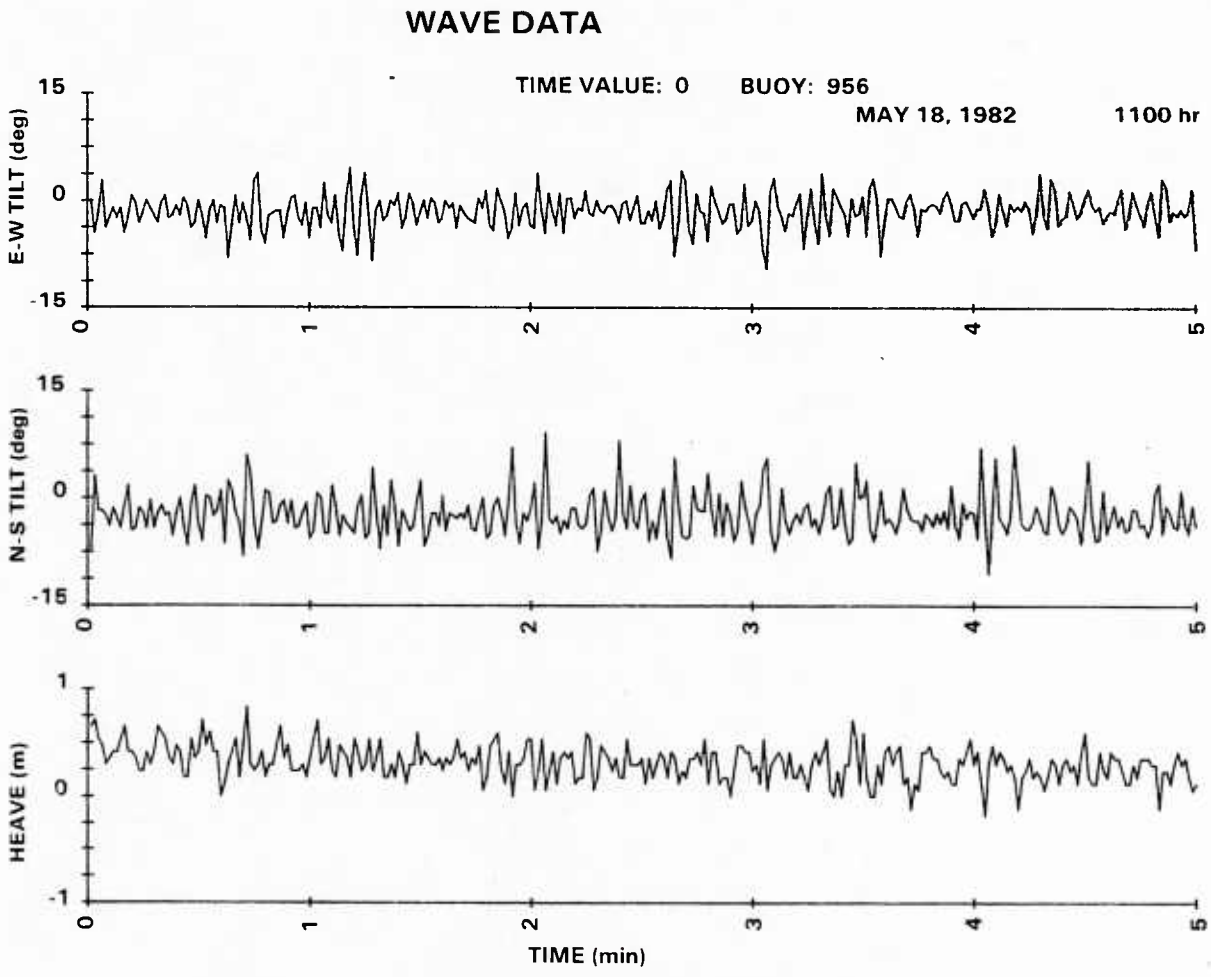

Figure 11. Plot of Wave Data Made Aboard USNS LYNCH

```
   1054 POINTS READ IN.

HEAVE
MEAN    STDV    SPIKES  RAW MAX  RAW MIN  FIN MAX  FIN MIN
131.1   1.36         0     161.     110.     5.83    -4.13
N-S TILT
MEAN    STDV    SPIKES  RAW MAX  RAW MIN  FIN MAX  FIN MIN
124.8   5.46         0     187.      86.    21.88   -13.63
E-W TILT
MEAN    STDV    SPIKES  RAW MAX  RAW MIN  FIN MAX  FIN MIN
128.7   4.64         1     214.      87.    15.59   -14.65

1054 GOOD DATA POINTS IN EACH SERIES.  SEGMENT LENGTH = 1024

REVISE MAXIMA/MINIMA
HEAVE
MAXIMUM READING:  4.86  MINIMUM READING: -3.74
N-S TILT
MAXIMUM READING: 21.88  MINIMUM READING:-13.63
E-W TILT
MAXIMUM READING: 15.59  MINIMUM READING:-14.65
```

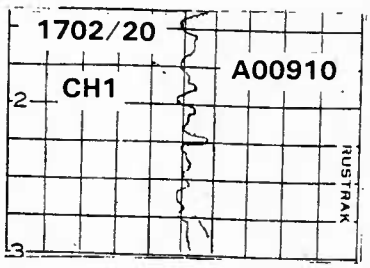


```
                        STATISTICS
                START:  5/20/82  --  17: 1:13

                NR WAVES:      189   PERIOD OF MAX HEIGHT:    8.0
                MAX PERIOD:   13.0   SIGNIFICANT PERIOD:      6.2
                MEAN PERIOD:   5.4   SIGNIFICANT HEIGHT:      4.9
                MEAN HEIGHT:   3.3   HEIGHT VARIANCE:         2.2
                MAX HEIGHT:    7.7   ROOT-MEAN-SQ HEIGHT:     3.6

                PROFILE OF MAXIMUM WAVE AT 1.00 SECOND INTERVALS
  -3.7    .6   3.9    .7  -1.8   -.1  -1.2   -.6   -.1   1.0

 FREQUENCY      CENTER        CENTER        ENERGY        MEAN        STANDARD
BANDNUMBER    FREQUENCY      PERIOD        DENSITY     DIRECTION     DEVIATION
      1          .038          26.6          7.85          128.          16.3
      2          .047          21.3          4.12          109.          18.6
      3          .060          16.8           .65           85.          12.6
      4          .075          13.3           .37           94.          14.5
      5          .097          10.3          1.55          100.          19.3
      6          .127           7.9          8.25          123.          14.6
      7          .171           5.8         14.18          181.           9.2
      8          .225           4.5          6.04          186.          10.7
      9          .292           3.4          2.78          187.          21.4
     10          .417           2.4           .71           94.          22.7
 ENVIRONMENTAL DEVICES CORPORATION
DIRECTIONAL WAVE BUOY DATA PROCESSING - 1017
       VERSION 1.4    - 1/82

WAITING FOR DATA.
```

Figure 12. Automatic Printout from Tarbell System at Block Island

The Tarbell program is constructed for the three ENDECO 956 output channels: (1) free surface, (2) E-W tilt, and (3) N-S tilt. From these data the program generates the statistics of the wave height characteristics. Also, using the tilt data, the program provides directional information as listed in the table at the bottom of figure 12.

When the ENDECO 1015 data are received, the free surface elevation data in statistics are valid since they are independent of the tilt information. Thus, there was a net hourly data summary of free surface elevation statistics provided, alternatively produced from the 956 and 1015 systems.

Figure 13 shows the mean and significant wave heights (i.e., the mean of the one-third highest waves) associated with the changing wind conditions. Superposition of significant heights on the wind speed time suggests a time lag of roughly 6 hours between the wind peaks and the maximum wave conditions. This indicates, as is further seen in the spectra, that the mean and significant heights represent a composite of locally wind-generated waves (seas) and swells.

The energy density values for each spectral band are summed in the Tarbell output (figure 12). It can be shown that the total variance of the record is proportional to the potential energy density of the wave field. These integrals, plotted as a function of time (figure 14), correspond, as expected, to the bimodal peaking of the significant and mean wave heights (figure 13) and the periods of maximum wind speed (figure 9).

The Tarbell auto spectra estimates offer a clearer picture of the changes in the wave field. Figure 15 shows six consecutive spectral estimates from the Tarbell data (the column "energy density" in figure 12), which display wave generation and decay over the period 19-25 May. Shown also in figure 15 are the wind speeds (U) for the times given, the total variance (value in parentheses), and the significant wave heights (SH).

For the period 19-20 May the freshening winds (figure 9) rapidly build upon the higher wave frequencies. From 20-25 May the spectral peak shifts steadily toward lower periods (redder frequencies) as the local winds diminish. However, the spectral energy continues to grow, peaking at 24 May (1500 hours-EDT) when the winds have become light. By 25 May (0300 hours) the energy is still large. The continuous energy growth well after the local winds have abated reflects the presence of the swells which, having been developed by the high winds of the cyclone to the east, have propagated into the test area.

The spectra, together with the wind variations, clearly demonstrate the complex cause and effects of wind-wave generation. The wave field (or its spectra) for any given instant is a product of the previous history of the wind and its origin; hence, the spectra do not particularly correlate with the instantaneous wind. Thus, for a gradual wind-wave buildup over a large area, local waves are growing, but soon swell is propagated into the area, creating a composite of sea superimposed on swell.

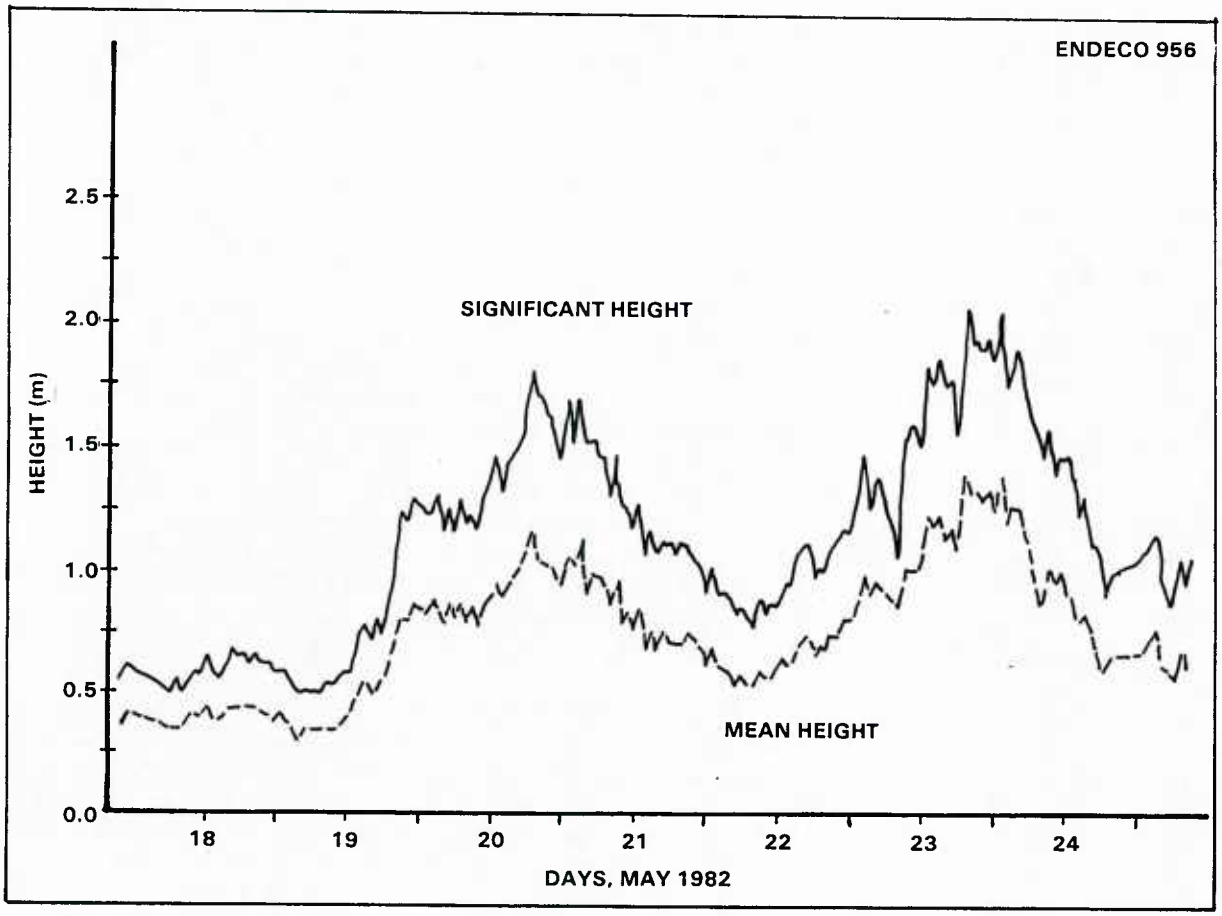

Figure 13. Significant and Mean Wave Heights During WEAP Experiment

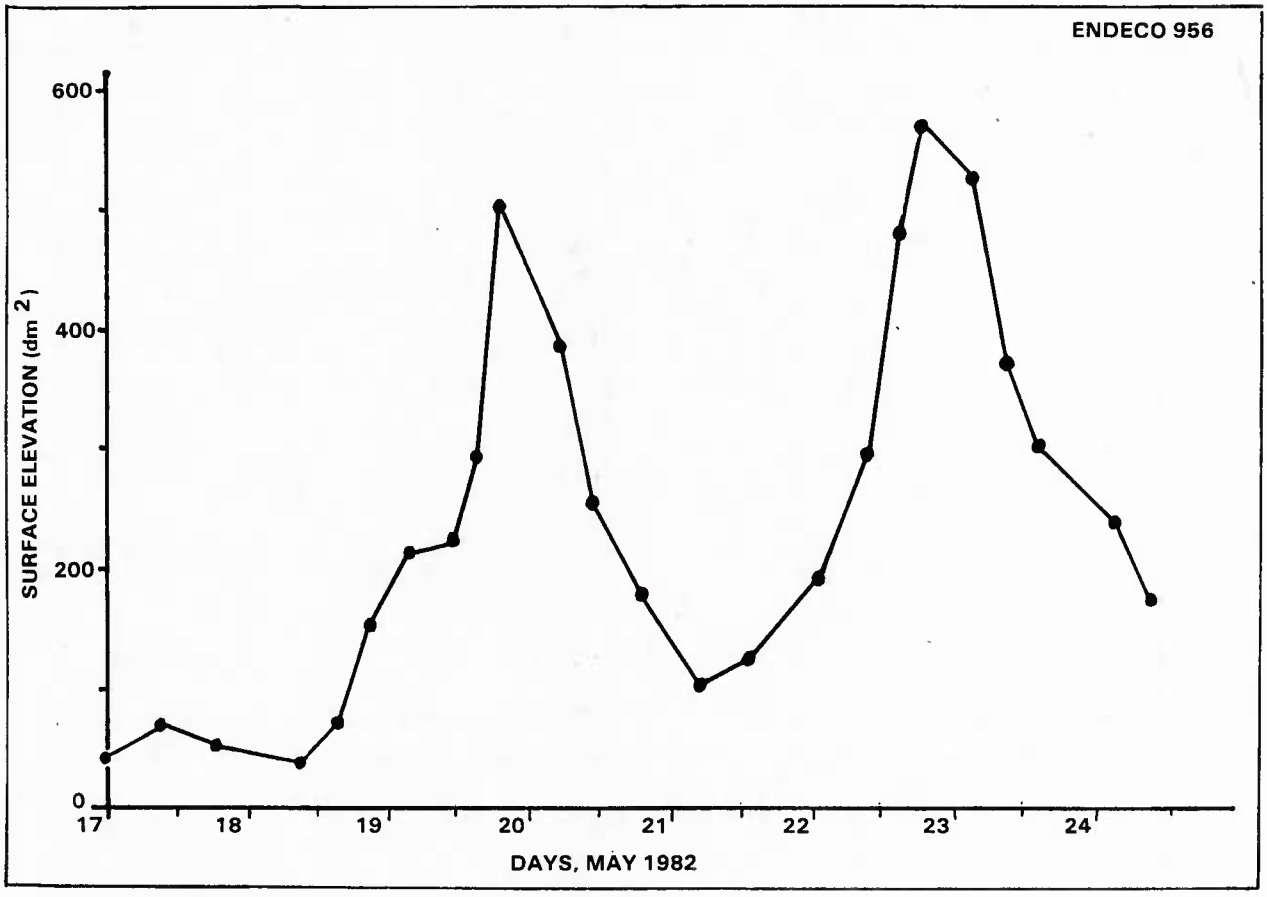

Figure 14. Variance of Vertical Displacement

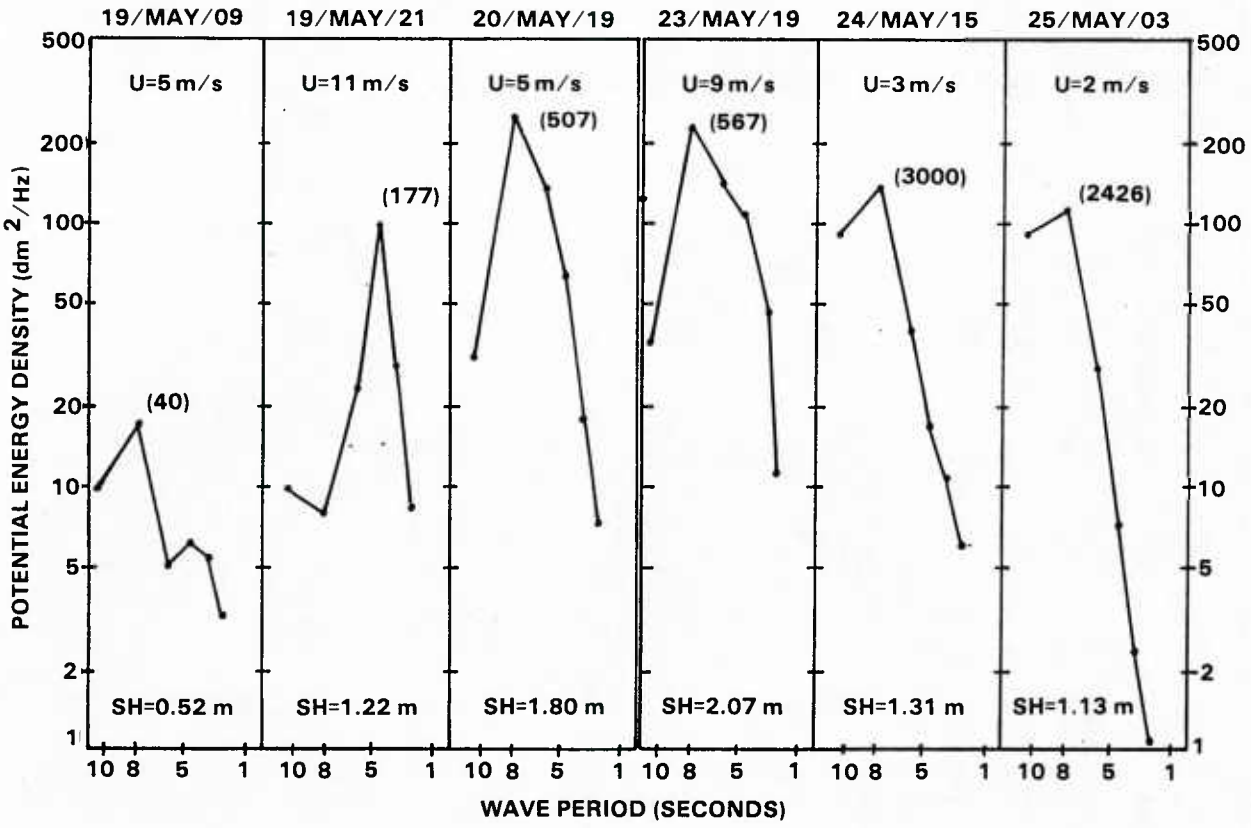

Figure 15. Selected Auto Spectral Density Distributions from the Tarbell Computations

An example of the directivity of wave buildup is shown in figure 16. The wave components at 1900 hours on 23 May are indicated by vectors radiating from the center of the diagram, with the vector length proportional to the component's energy. The vectors suggest the average direction of propagation of the waves of the particular frequency (period) band. The measured wind vectors are shown for times 0, 3, 6, and 9 hours prior to the record. The small waves having a period of 3.4 seconds (0.29 Hz) appear opposite the most recent wind vector, and those having a period of 10.3 seconds (0.10 Hz) appear opposite the wind vector of 9 hours previous. This wind-wave direction diagram, although crude, is suggestive of the ability of the Type 956 directional wave-track buoy to portray wave generation.

The analysis of the wave/current data recorded aboard the USNS Lynch produced both raw data and auto spectra plots. The first sample record is from 18 May at 1200 hours (figure 17) at which time the wind speed was light (5 meters/second and the seas light to moderate (figures 13 and 14). The upper two portions of figure 17 show the raw data plots of the current meter direction and speed, and the bottom portion shows the free surface height (obtained from the double integration of the accelerometer output). The upper box contains the following information pertaining to the wave records: serial No., data, time, record length, sampling interval (either 0.5 or 1.0 second), wave height, variance, significant height (mean of the highest 1/3 of the records), wind speed and direction, and current variance. The wave height units are decimeters (dm), and the current speed is in centimeters/second (cm/s).

The auto spectrum for the record is shown in figure 18 along with the pertinent information. The spectrum displays weak energy distribution, with a small peak at about 0.13 Hz (or 7.7-second period). The small wave energy corresponds to the small waves estimated by the Tarbell analysis (figure 13).

The next record, from 23 May at 2000 hours (figure 19), represents the largest waves observed, as indicated by the Tarbell records (figure 13), and at the end of the period the highest wind speeds (figure 9). Perturbation of the buoy motion is obviously due to the large surface waves; this is reflected in the current speed record as speed excursions from 30 to 45 centimeters/second. This contamination of current speeds by the buoy motions is discussed further in the next section).

As expected, the spectrum of the large waves is highly energetic (figure 20), with a large peak at about 0.14 Hz (i.e. 7.1-second period). The wave energy is highly narrowbanded since the waves were produced locally from strong winds persisting from the east quadrant on 23 May.

The data from this buoy will be analyzed by a more fundamental FFT technique developed by LeBlanc and Middleton (reference 9) which is based upon the original work of Barber (reference 10) and refined by Longuet-Higgins, Cartwright, and Smith (reference 11). The method of obtaining directional spectra was applied to data from a wave tilt buoy developed at the National Institute of Oceanography (now the British Institute for Oceanographic Sciences). The technique involves finding the first five Fourier coefficients of the directional energy spectrum from free surface height together with X-Y tilt data. This technique will be utilized in further data analysis of the Type 956 wave-track data.

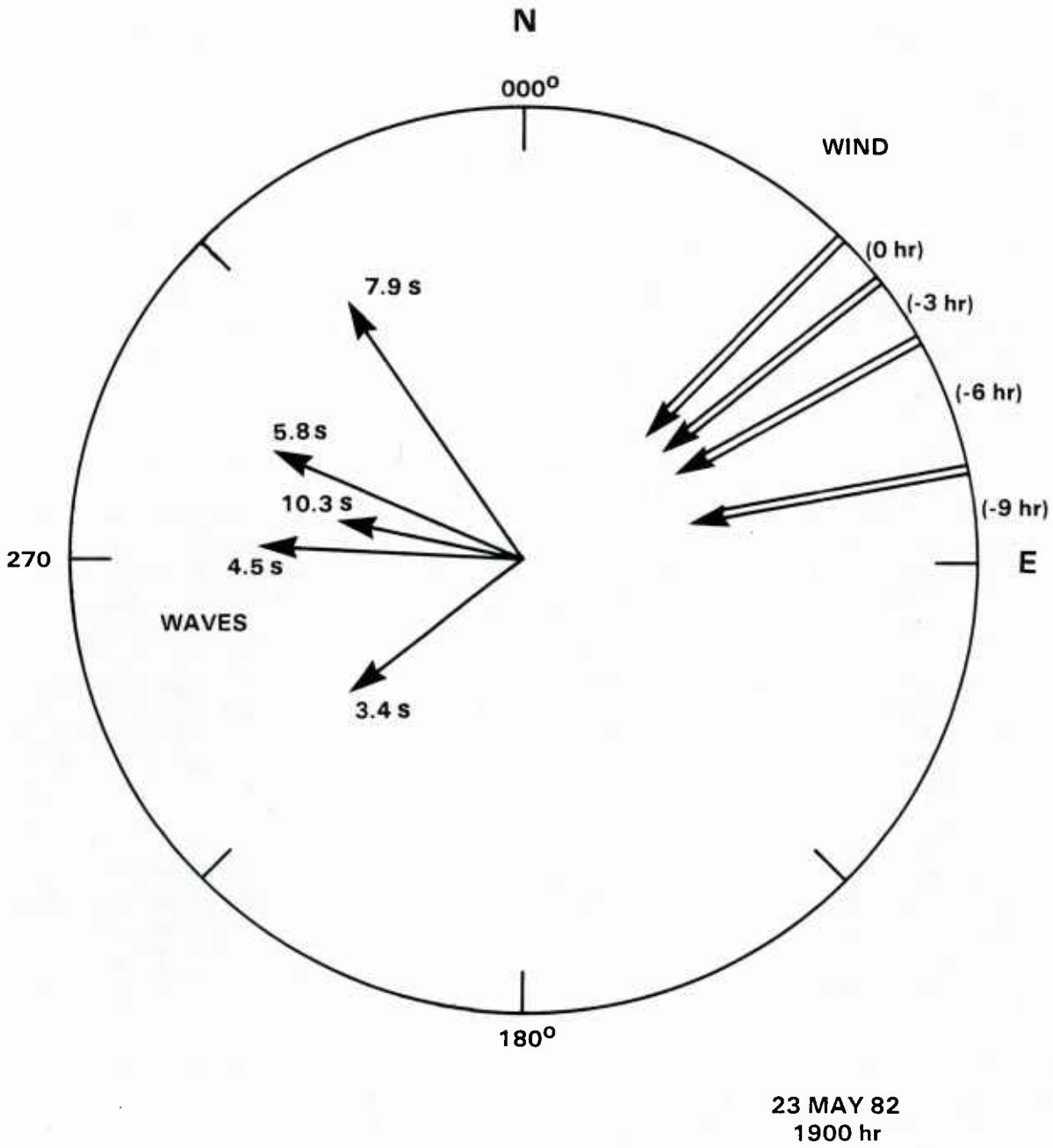

Figure 16. Wind and Wave Direction Vectors

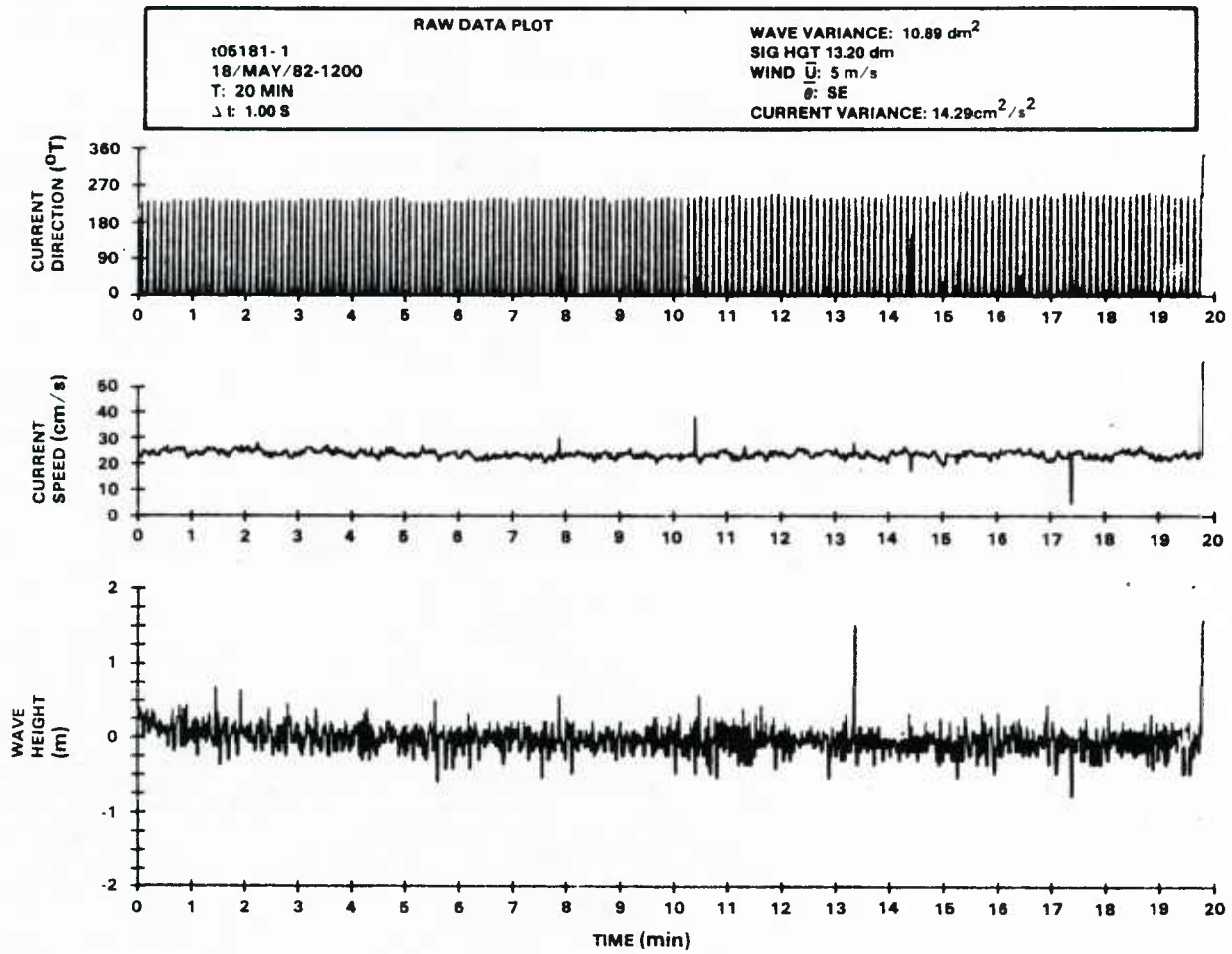

Figure 17. Raw Data Plot for the 18 May Record from the NUSC Wave Analysis Program Showing Current Direction/ Speed and Wave Profiles During Low Wave Conditions

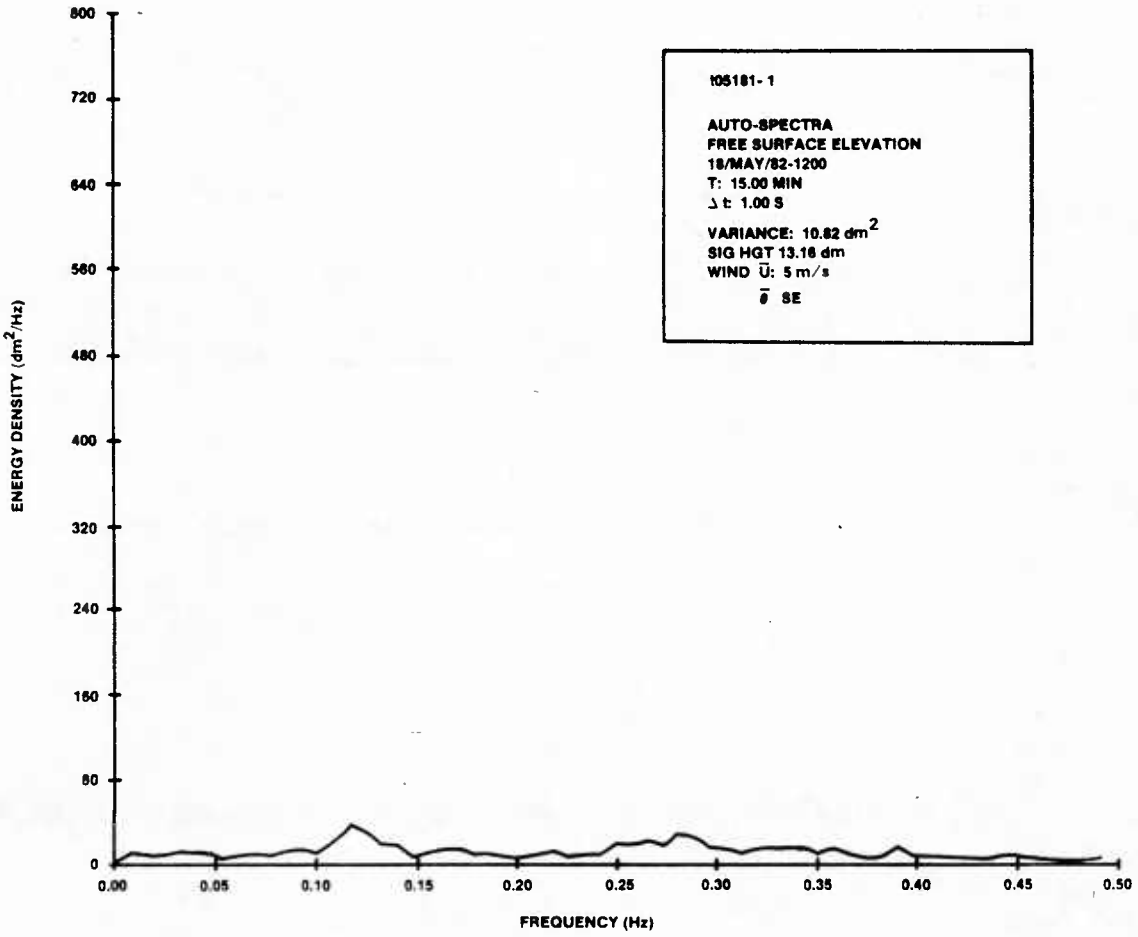

Figure 18. Spectrum for Wave Conditions Shown in Figure 17

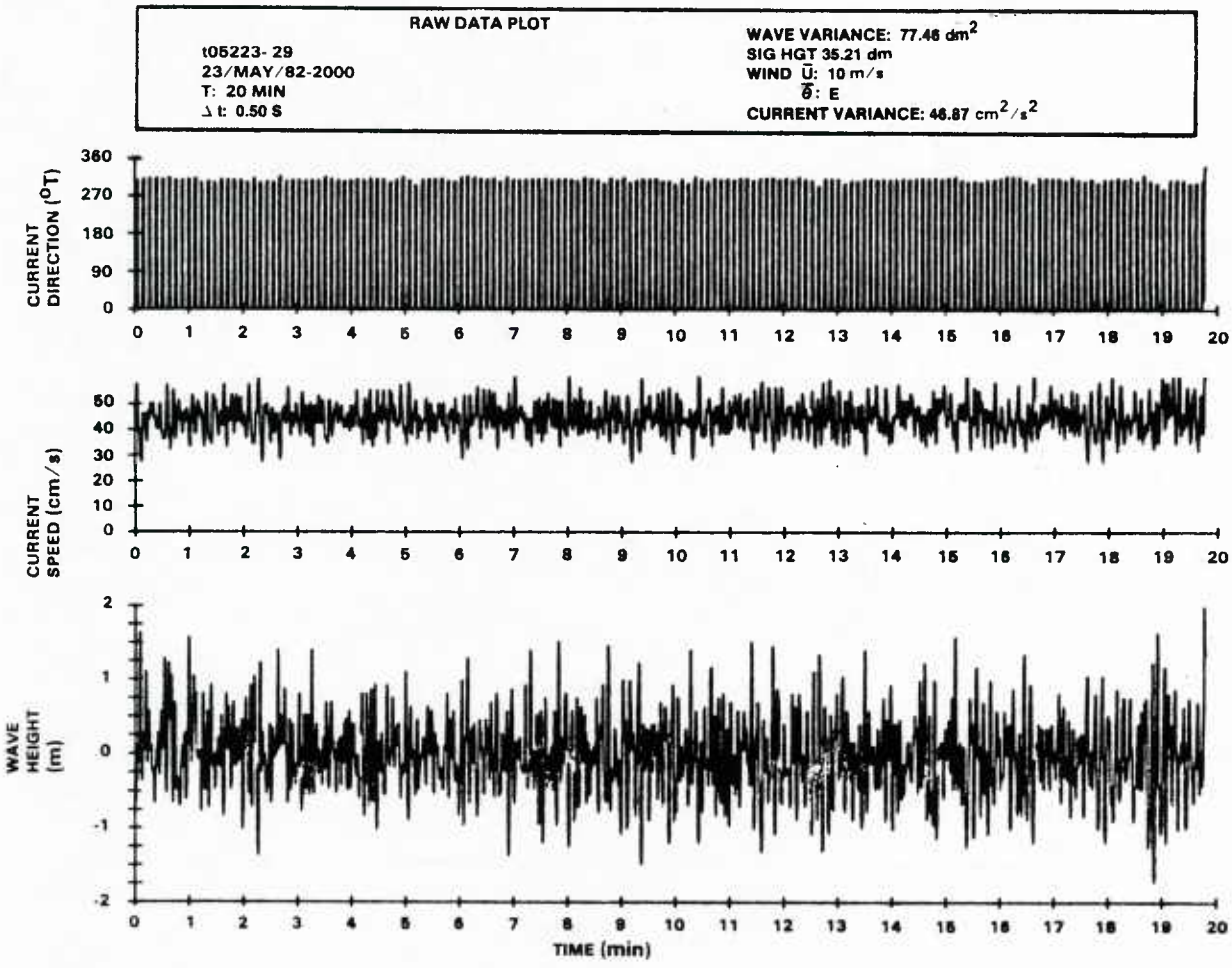

Figure 19. Raw Data Plot for 23 May Record Showing Relatively High Wave Conditions

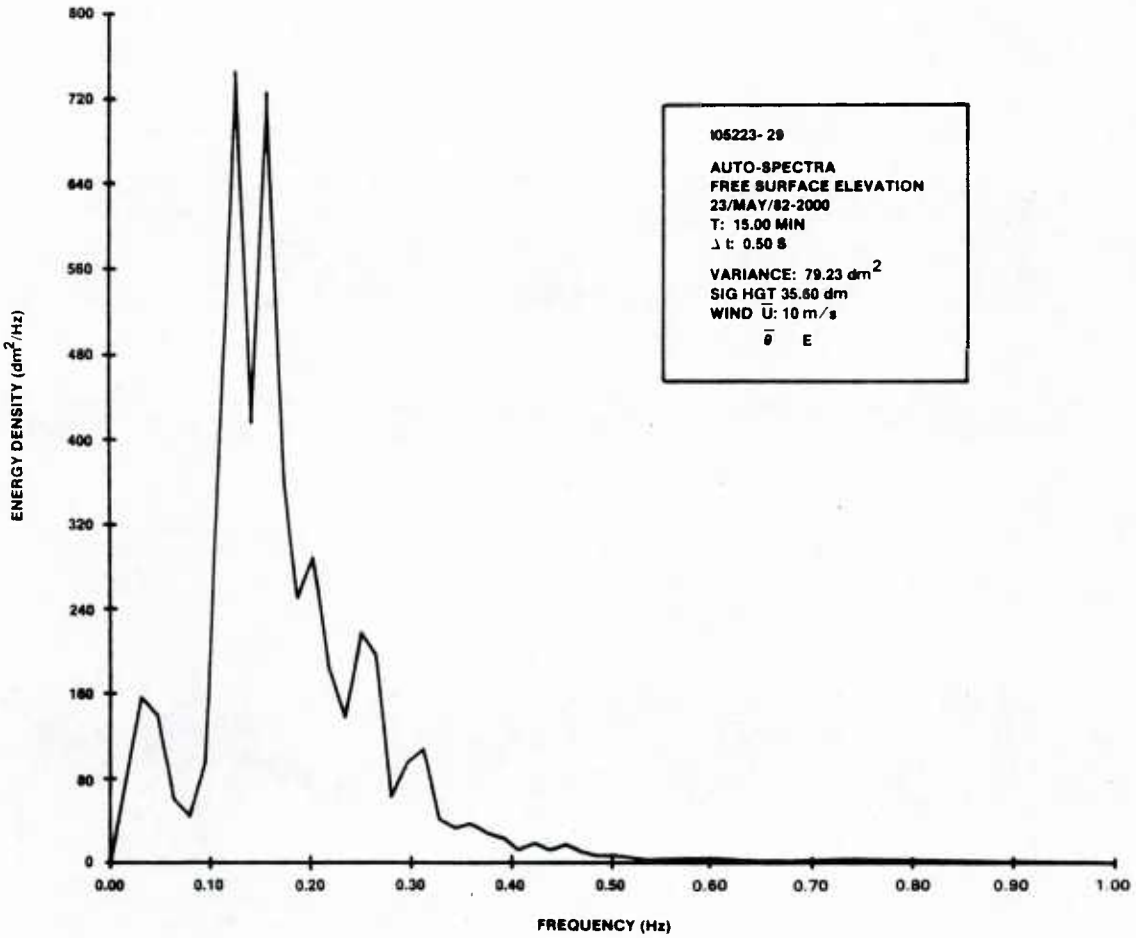

Figure 20. Spectrum of Wave Data Shown in Figure 19

CURRENT DATA

The current speed and direction from the WEAP operation area were obtained using the ENDECO 1015 system with the current meter at 5 meters depth beneath the wave-track surface buoy located 700 meters east of the USNS LYNCH (figure 1). Data were received both at the LYNCH and at the Block Island Field Station. A sample of a 20-minute telemetered current record is shown in figure 21. This sample was made during wind speeds of 8-9 meters/second with about 1.2 meters significant wave heights (figures 9 and 13). Some of the wiggles on the direction and speed traces may be due to surface buoy oscillations perturbing the current meter. However, the records seem quite stable; i.e., the current flowed consistently southward (180° T), and the speed was 15-18 centimeters/second.

Cursory visual examination of the actual speed and direction records, particularly those reflecting periods of high wind or wave conditions, revealed no obvious biasing of the current data due to vertical heave of the surface wave buoy. Therefore, no attempt was made to filter the records at surface wave frequencies, and only the raw data are discussed below. (Further examination of possible bias due to buoy motions is presented in the next section)

At Block Island the Type 1015 data were processed on the Tarbell computer, which was programmed to analyze the three channels of the Type 956, i.e., heave and the two tilt channels. In substituting current speed (channel 2) and direction (channel 3) for the tilt data, the program provides mean values of the two variables. However, the direction is internally sampled only during 1 second out of every 4 and reads zero otherwise. Thus, the direction record from the Tarbell was unusable, and the direction data had to be derived from the LYNCH, which unfortunately had record gaps because of intermittent magnetic tape rewind and adjustment periods.

The available direction and speed data were averaged for each 20-minute sampling interval and plotted at 10 minutes after the hour at each 2-hour interval (figure 22). The direction data, in spite of the missing points, display a strong rotary tidal nature of M_2 variations. (The excursion from 360° T to 0° T is indicated by the broken lines.) The speeds, however, appear atypical since they display generally a single maximum per tidal period instead of the double maximum of a sinusoidal character. The speed ranged from 5-70 centimeters/second and averaged 27.6 centimeters/second. This was in agreement with observations in Rhode Island Sound made by Shonting (reference 12).

The rotary character of the tidal motions is displayed by the LaGrangian Hodographs (head-to-tail vector diagrams) in figure 23. The 20-minute average speeds and directions are assumed to be representative over 2-hour intervals (since the 20-minute sample was obtained every 2 hours). The mean transport and trajectory of motion changes from a clockwise quasi-circular motion between 18 May at 0400 hours and 21 May at 0600 hours, to a strong westerly set between 21 May at 1400 hours and 22 May at 1400 hours. This coincides with persistent E and ENE winds (figure 9) which appear to generate surface current moving westward.

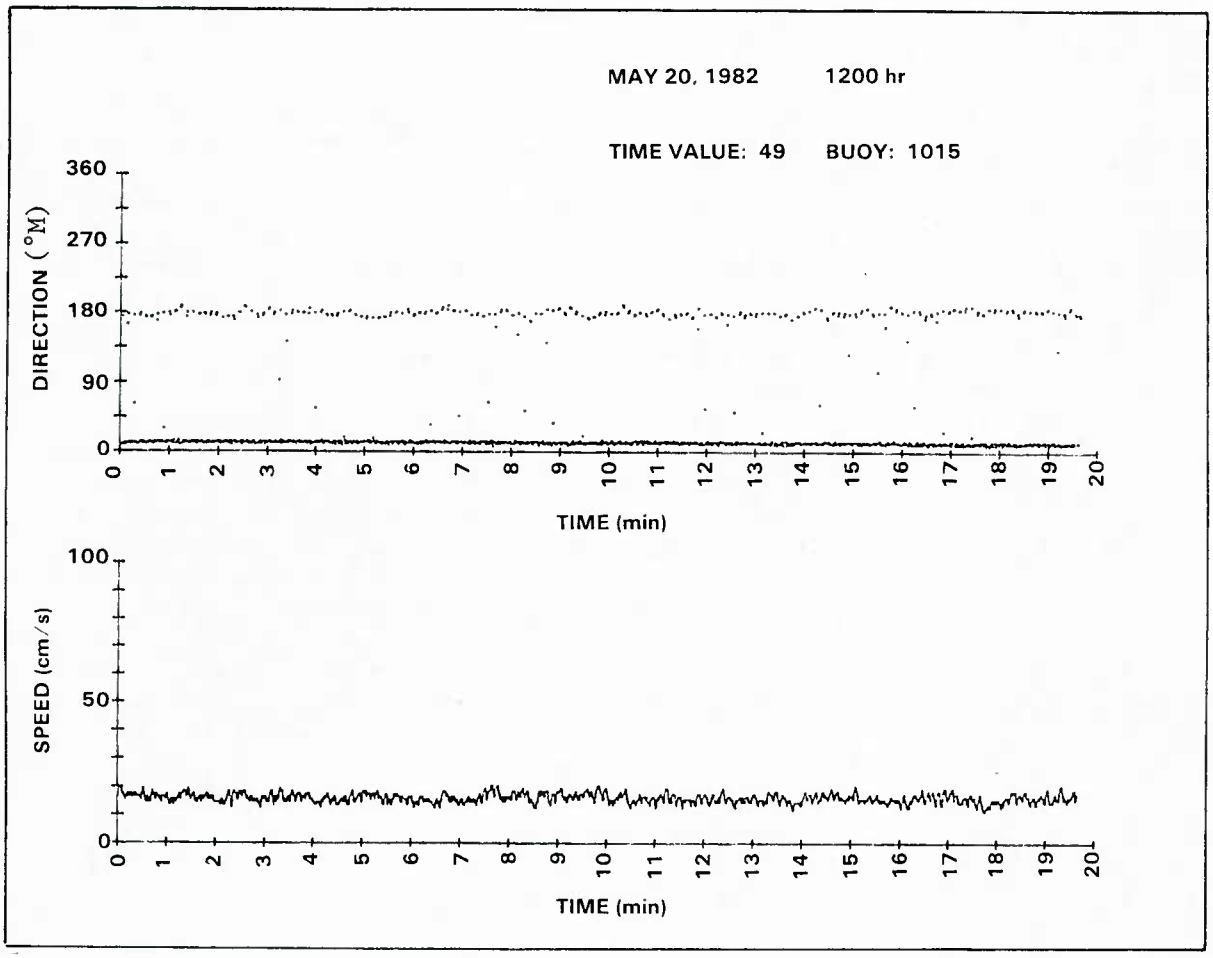

Figure 21. Sample of Current Speed and Direction Obtained on HP 9825A Aboard the USNS LYNCH

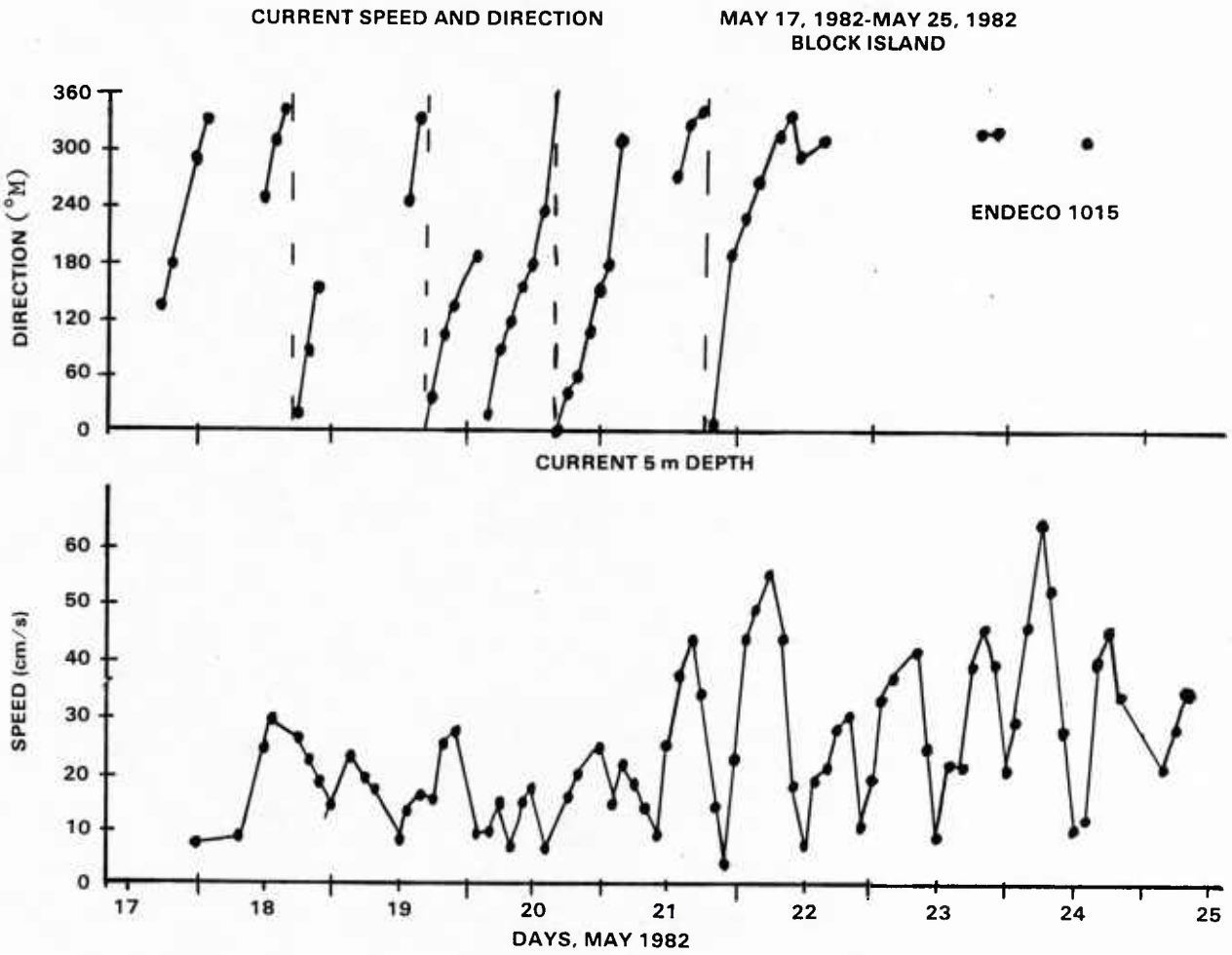

Figure 22. Current Speed and Direction for the WEAP Experiment

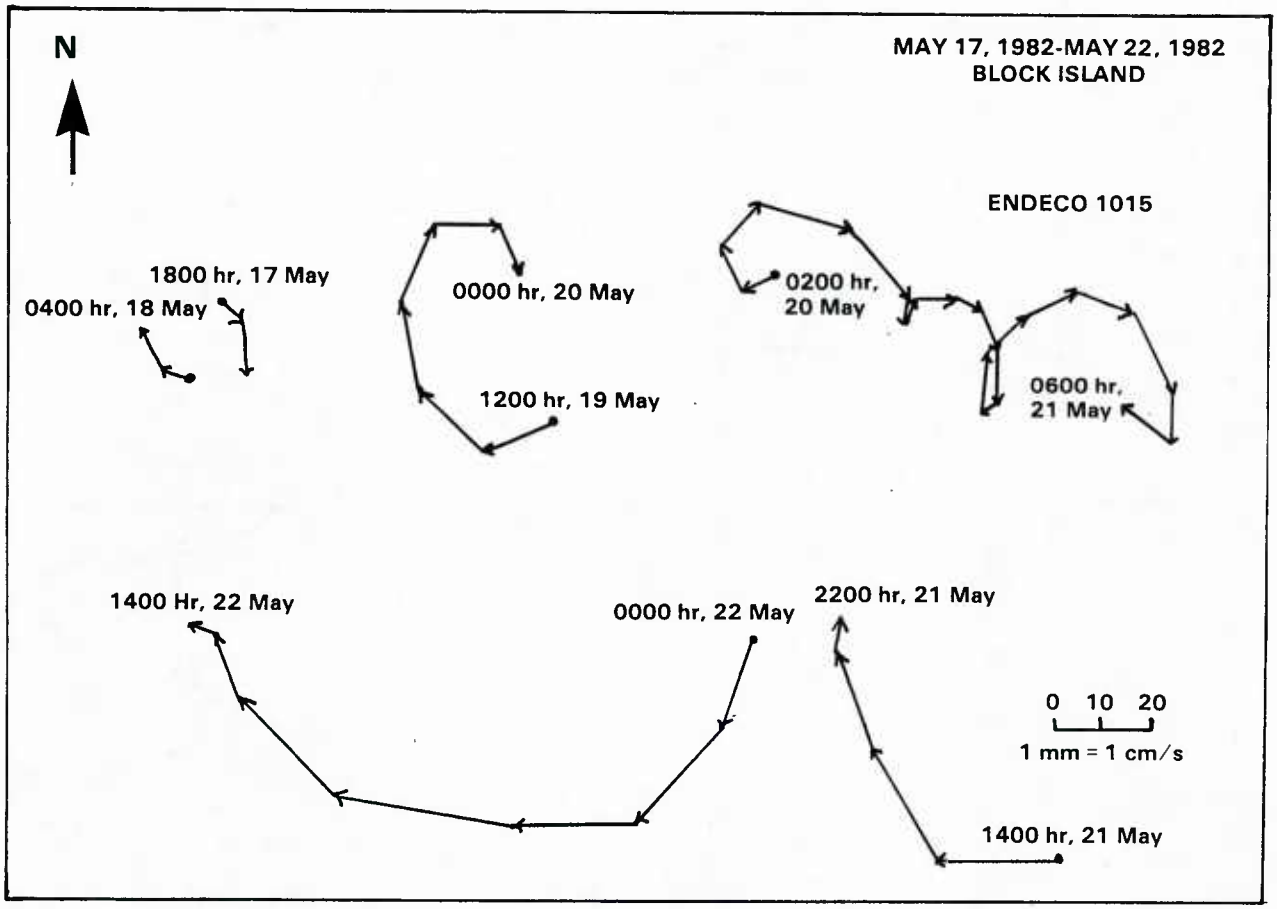

Figure 23. Lagrangian Hodographs of Current Data

EFFECTS OF BUOY MOTIONS ON CURRENT OBSERVATIONS

The ENDECO Type 1015 wave-track/current meter buoy incorporated a Type 948 wave body at the surface with a current meter tethered to the wave buoy mooring line some 5 meters beneath the surface. One of the objectives of the observations using the Type 1015 system was to determine possible bias to the current data caused by perturbations on the current meter arising from surface wave motions. Thus, the tethered instrument could be affected by vertical heave imparted to the mooring line by oscillatory movement of the surface float in the wave field and by the orbital motions of the waves themselves. This effect is borne out by measurement as is shown in figure 19 where clear contamination of the buoy motions produced by larger waves shows up in the current speed record.

The geometry of the tethered current meter suspension is designed to minimize the translation of motions of the mooring line to the current meter. Normally, the "mooring line" is a taut cable with perhaps several instruments attached at various depths and is connected to a subsurface or surface float. The use of the horizontal 1.6-meter tether to the current meter served to decouple vertical or vibration motions of the mooring line from the meter body.

A theoretical model study was made of mooring systems for a tethered current meter by Triantafyllou and Salter (reference 13). The analysis concentrated on the dynamics of the mooring cable in both taut and slack catenary configurations. Forces and tensions on the cable were estimated for various mooring lengths, tether points, tether lengths, cable diameters, cable specific gravities, water depths, and current speeds.

The study delineates the relevant parameters in the dynamic system and assesses the various force and tension distributions associated with different wave spectra conditions. The conclusions recommend the use of a slack mooring in lieu of a taut system for the greatest stability of the tethered current meter. The taut system, because of its tendency to have a snapping effect when the currents were weak, increased the effects of wave motions to cause instability in the tether line.

Unfortunately, little attention was paid to the possible perturbations on the current meter per se; i.e., the equations were not integrated to evaluate the error in the current associated with the cable and wave motions. The study does, however, offer a basis for engineering analysis of cable dynamics in various wave and current environments.

A measure of the decoupling of the tethered instrument from a vertical cable was obtained in a tank test conducted by ENDECO at the David W. Taylor Naval Ship Research and Development Center (DTNSRDC) in Bethesda, MD (reference 14). The test system allowed the current meter tether point to be oscillated vertically at various amplitudes and periods while it experienced different flow speeds in the water channel (figure 24). The flow speed was measured independently and compared to the current meter output using oscillation periods of 3, 6, and 9 seconds, amplitudes (half ranges) of 40 and

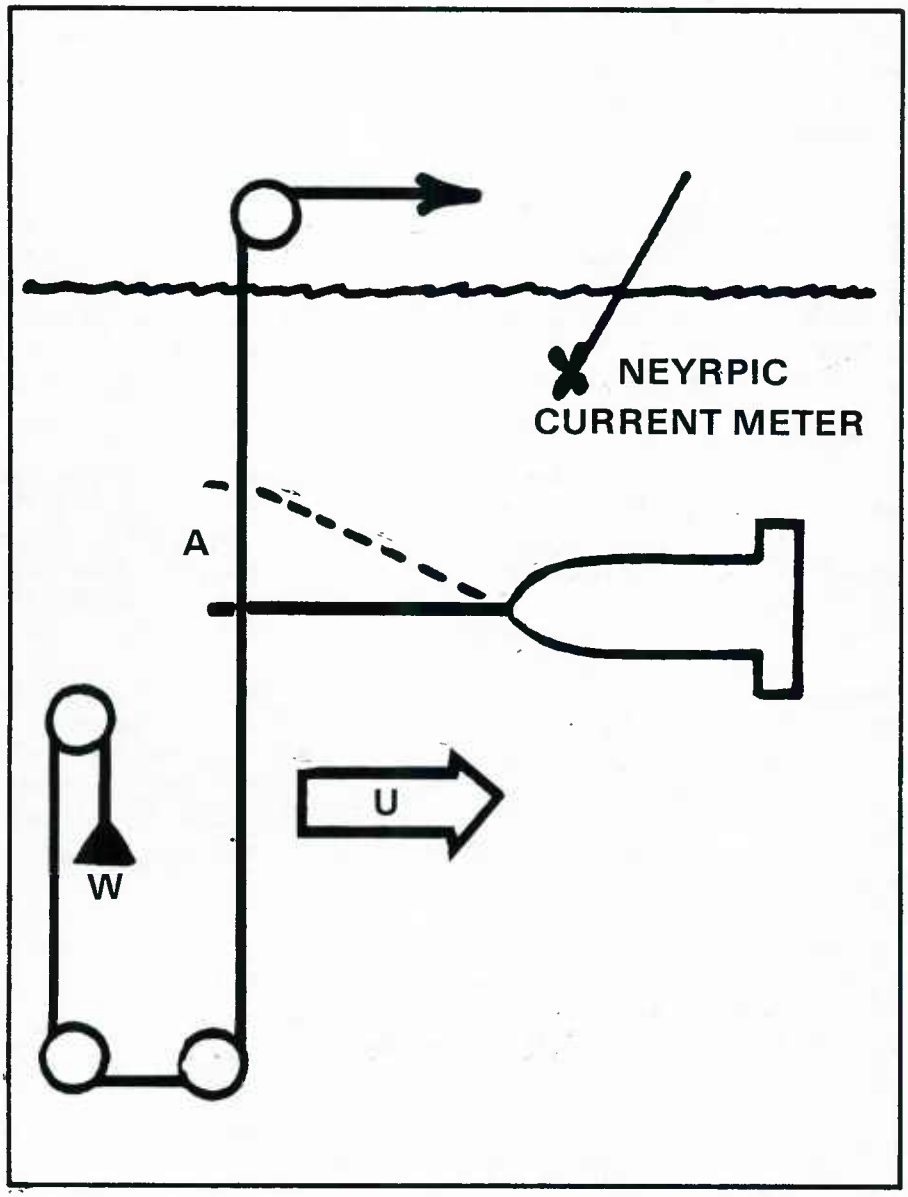

Figure 24. Test Configuration for Tank Test of Current Meter

63 centimeters, and mean flow currents of 39 - 64 centimeters/second. The results are summarized in figure 25.

The error due to the tether oscillation ranged from 3.2 to 8.0 percent and appeared larger at the 6-second period than at the 3-second period. Unfortunately, the current speed range is small, and error effects below 39 centimeters/second were not presented. The report concludes, however, that the effects of vertical motion upon the measurement of horizontal current appear minimal.

Unlike the typical taut-line current meter mooring system referred to above, the Type 1015 wave-track/current meter buoy utilizes a slack mooring line of about three-to-one scope, with the current meter tethered at about 5 meters beneath the surface; this distance is necessary so that the surface wave buoy can freely oscillate in the wave field. Although Triantafyllou and Salter (reference 14) suggest that a slack cable has better damping characteristics than a taut moor, they do not recommend placing the instrument near the surface. Clearly, a loose catenary mooring line could allow the current meter more freedom to oscillate vertically than would a taut mooring cable (at least in shallow depths (< 100 meters) where the net cable stretching is minimal). Thus a price may be paid in the quality of current data by attempting to measure current so near to the sea surface in the presence of wave orbital motions. On the other hand, it may be that under moderate wave conditions a 5-meter tether depth is sufficient for the exponential decay of wave amplitude to minimize the perturbations, and that the natural damping of the slack catenary may dominate the tether system.

Consideration of the geometry of the tethered current meter system allows some crude insight as to the current meter motions imposed by the surface waves. A simplified picture of at least the kinematics of the buoy-current meter system is given in figure 26. The wave buoy is attached to the mooring line at point Q which is the center of horizontal drag for the mean wetted surface (including the lower hemisphere of the buoy, the shaft, and the accelerometer housing, figure 2). Thus, for a mean surface current, the drag on the moored buoy should contribute minimal net tilt.

The current meter is attached to the mooring line by a neutrally buoyant tether line of length L at point P. The current meter is weighted so that it is neutrally buoyant (i.e., its buoyancy b is equal and opposite to its weight W). The instrument is also trimmed so that as the drag of the horizontal current U_c imparts upon it a horizontal pull, the longitudinal axis of the current meter coincides with the horizontal tether.

The wave buoy, in response to the surface waves, has a vertical amplitude of displacement, say δ_s, which is felt at the tether point as a vertical oscillation given by

$$\delta(t) = \delta_o \sin\omega_o t, \qquad (1)$$

where δ_o is the amplitude (and $\delta_o < \delta_s$, since the catenary is likely to absorb some of the surface motion) and ω_o is an arbitrary surface wave frequency where

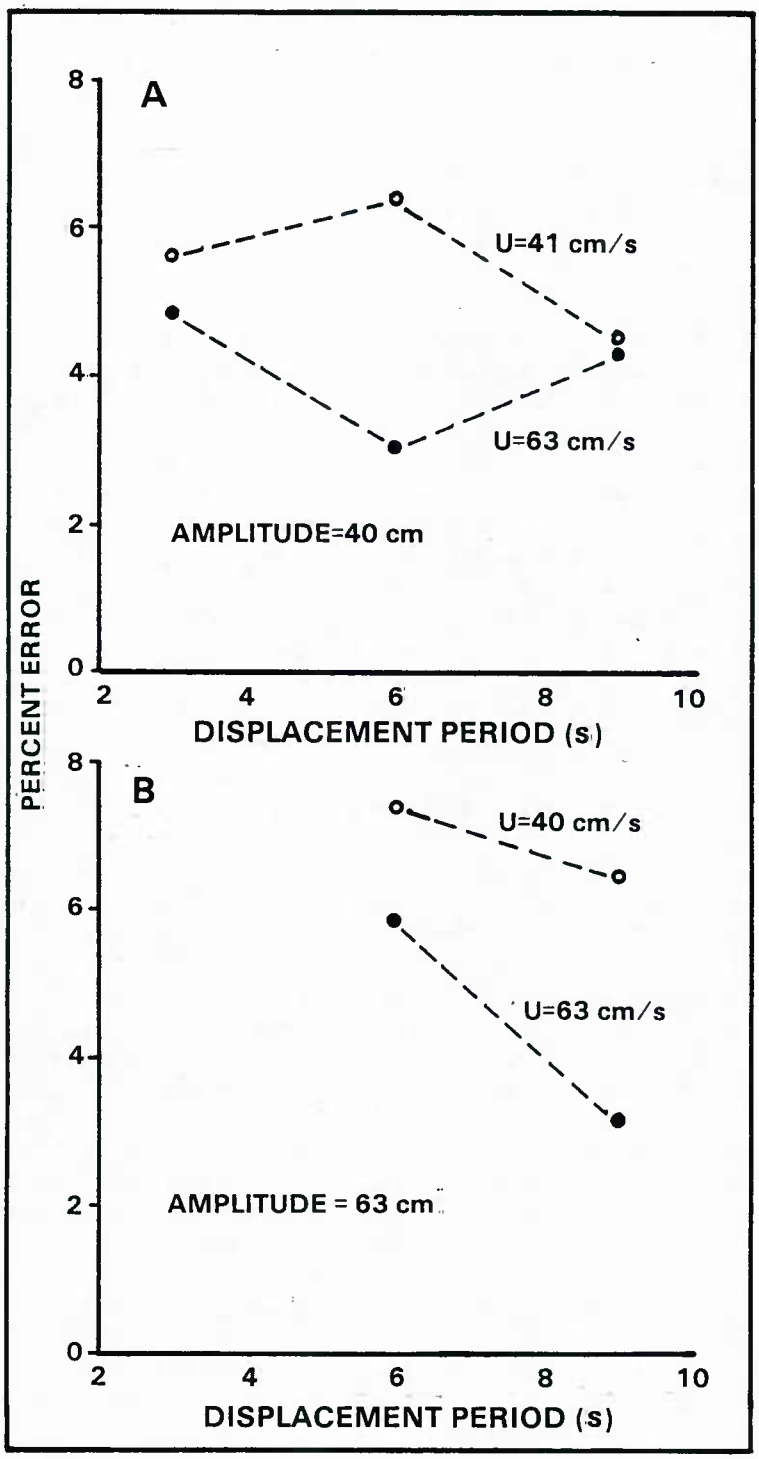

Figure 25. Positive Error in Current Measurement for Amplitudes of 40 and 63 cm and at Two Towing Speeds

$$\omega_o = \frac{2\pi}{T_o} , \qquad (2)$$

T_o being the period (s).

The problem is to estimate the horizontal current U_c sensed by the current meter as the tether point P is oscillated as defined by equation (1). The analysis is made with the following assumptions:

1. The current drag acts as a restoring force opposing the forward acceleration caused by the P tether point moving up and down. Thus, as the tether rises and falls, the tether is always stretched out.

2. The orientation of the current meter remains horizontal.

3. The variable force on the current meter causes it to move approximately along the tether direction toward the upper and lower limit of the vertical excursions of the tether point.

Without these simplifying assumptions the analysis becomes hopelessly complicated since the precise motions of the current meter are dependent upon instantaneous drag and accelerations and torques related to different flow angles of attack. Further, it is felt that with the simplification the gross perturbations are properly estimated.

Referring to figure 26, the current meter tether point P is elevated a distance δ_o, at which time the tether of length L makes an angle Θ with the horizontal equilibrium position. When the tether point has reached a point δ_o from equilibrium point P, the current meter must be displaced at least a distance ΔL in the new direction of the tether (figure 27). The horizontal component of ΔL is given by

$$\Delta x = \Delta L \cos\Theta = L(1-\cos\Theta). \qquad (3)$$

If it is assumed that the vertical displacement $\delta(t)$ given by equation (1) is due to a passing ocean wave, then for a full cycle oscillation the meter would be accelerated over the distance $+\Delta x$ during the first and third quarters of the wave period T_o. During the second and fourth quarters, the instrument is allowed to reverse its displacement, being carried back $-\Delta x$ by the mean current. This fluctuating velocity is approximated by

$$u(t) \cong \frac{d\Delta x}{dt} = \frac{d}{dt}\left[L(1-\cos\Theta)\right] . \qquad (4)$$

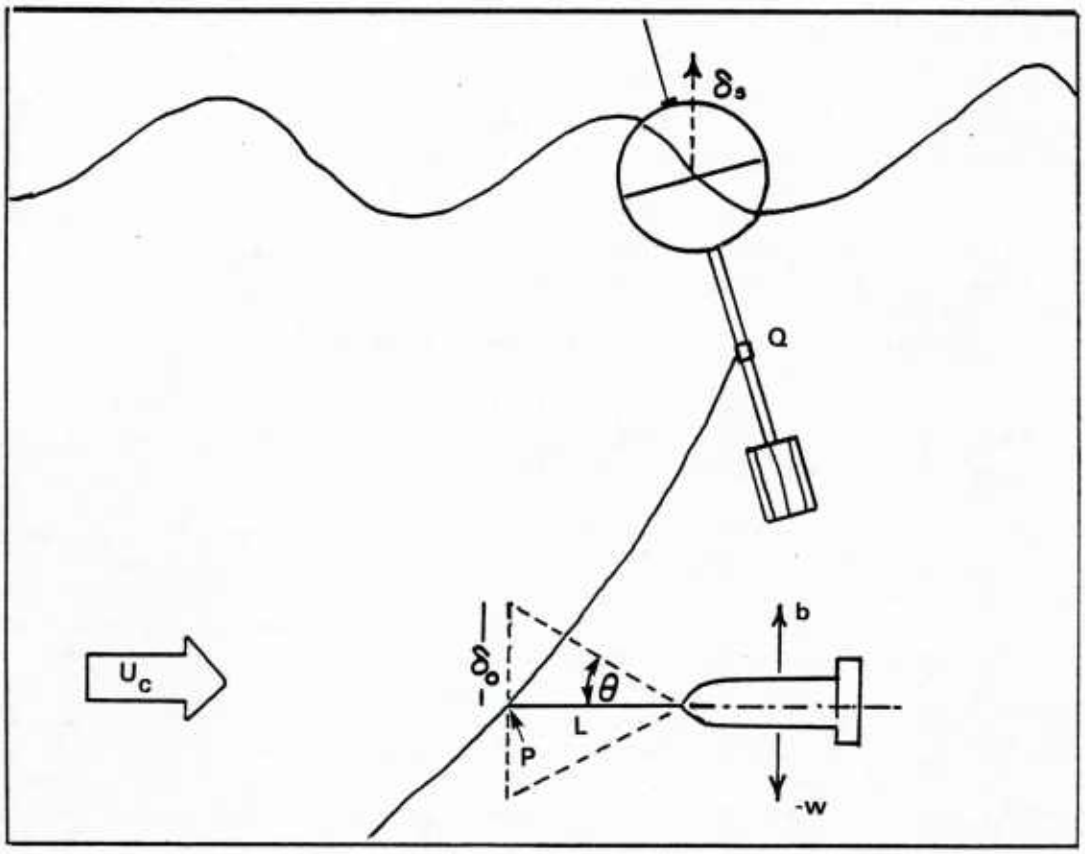

Figure 26. Configuration of ENDECO Current Meter Attachment to Wave-Track Buoy Mooring Cable

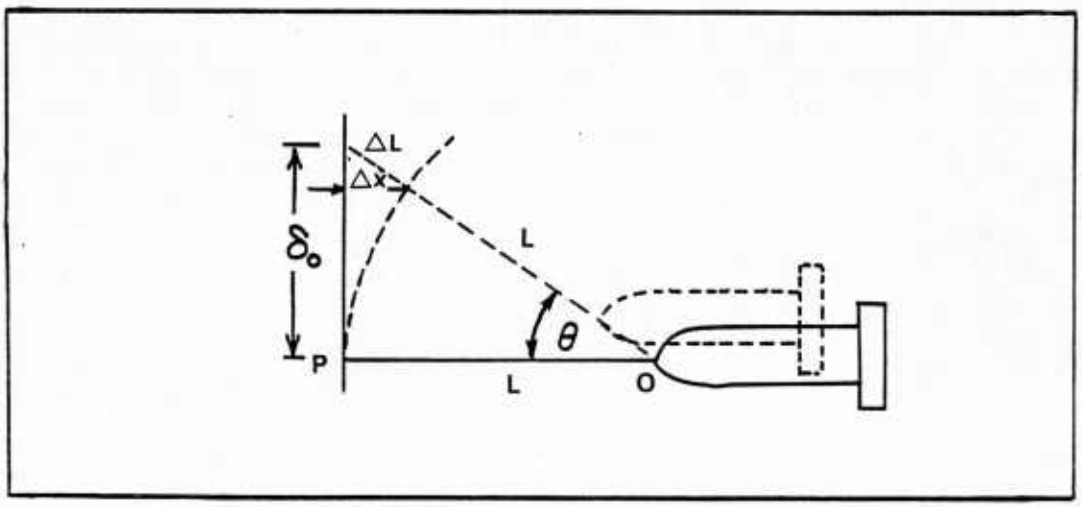

Figure 27. Geometry of Displacement of Current Meter as the Mooring Line Oscillates Vertically

By noting that Θ is a function of time from the relation

$$\tan\left[\theta(t)\right] = \frac{\delta(t)}{L} \quad ,$$

and with a little manipulation and the use of mathematical tables, one arrives at

$$u(t) \cong \frac{d\Delta x}{dt} = L^2\ \delta_o\ \omega_o \sin\left\{\tan^{-1}\left[\delta_o \frac{\sin\omega_o t}{L}\right]\right\} \frac{\cos\omega_o t}{L^2+\delta_o{}^2\ \sin\omega_o t} \quad . \qquad (5)$$

This rather imposing relation is plotted in figure 28 using the values of L, δ_o and ω_o indicated. Note that the frequency of u(t) is twice the wave frequency ω_o. During the quarter wave period excursion (Io/4), the velocity u(t) starts at zero, reaches a maximum, and then returns to zero when $\delta(t) = \delta_o$.

If assumption 1 holds, then the net contribution of u(t) to the non-wave current is negligible since

$$\frac{1}{nT_o} \int_o^{nT_o} u(t)dt = o; \quad n = 1, 2, 3, \ldots . \qquad (6)$$

Clearly, the true perturbation of the waves is not likely to average out completely; however, it should be small for values of $\delta_o/L<1$, and further perturbations of the tether motions should show up in the current records as a spectral peak at twice the wave frequency.

Quantitative measurements of the current meter motions (and hence potential bias of the current data) are not available. However, a rough assessment of data bias may be obtained by comparing the character of the current records with the surface wave conditions that directly control the surface buoy motions and hence may affect the tether and current stability.

During the 7-day WEAP experiment, wave conditions varied substantially; significant heights ranged from 0.5 - 2.1 meters (figure 13). Plots were made of simultaneous wave and current records at times of diverse sea conditions (figure 29). Also shown are the correlation coefficients between the wave heights and current speeds, the significant heights (SH) and the variances of the two signals - these being proportional to the kinetic energy of the waves and current fluctuations.

The 19 May record is representative of a period of light winds and small waves. Visual comparison of the heave correlation coefficient of -0.06 suggests negligible perturbation of the current meter by the ambient wave motions.

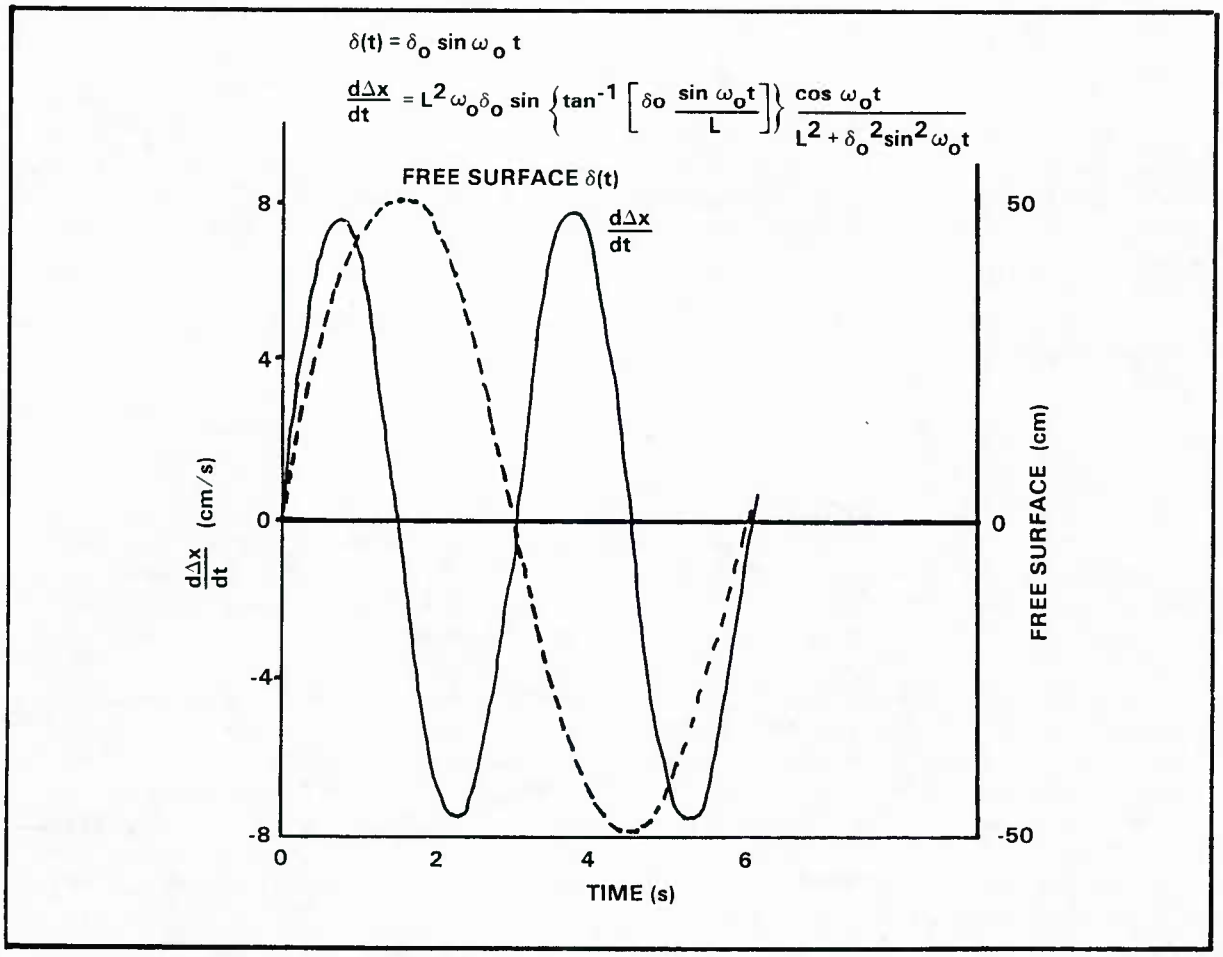

Figure 28. Model of the Free Surface Fluctuation and the Horizontal Current Response

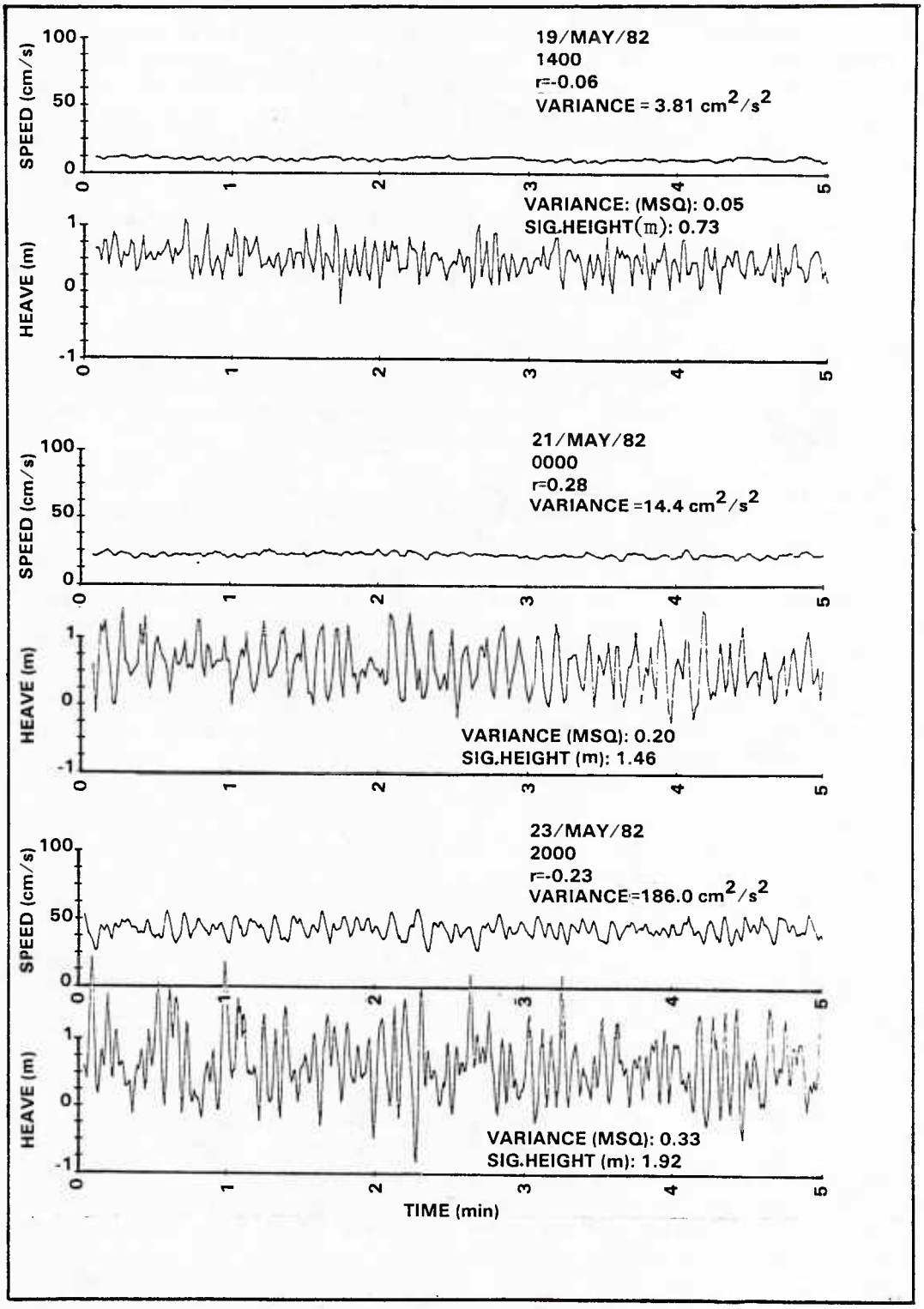

Figure 29. Samples of Recorded Current Speed and Heave Displacement During Different Wave Conditions. (Shown also are the correlation coefficient r, the variances of each signal, and the significant wave height.)

The 21 May record indicates that moderately high waves were generated during the previous 24 -30 hours from SSW winds of 7 - 10 meters/second (figure 9). This direction has a fetch over New York Bight of over 250 kilometers. The current record contains wavelike oscillations that appear to correlate with the heave record, as indicated by a correlation of +0.28.

The 23 May record (figure 13) represents the highest waves encountered. These waves are associated with ENE winds over a 50 - 100 kilometer fetch; and with speeds of 8 - 11 meters/second during the previous 24 hours, the winds generated waves with significant heights of 1.9 - 2.1 meters.

The speed record with a large variance of 187.0 cm^2/s^2 appears strongly perturbed by the large surface waves (figure 25). The correlation shift between the rise of the wave surface and the speed perturbation opposed to the response is depicted on the 21 May record.

The large increase in current meter response and change of sign of the correlation from the two records suggest that differences in the dynamic coupling occur between the two records. Also, the large increase in current record variance from 14.46 cm^2/s^2 on 21 May to 185.96 cm^2/s^2 on 23 May, while the wave variance only increased from 0.20 m^2 to 0.33 m^2, suggests a nonlinear effect of the wave motions upon the current meter perturbations. This effort was further examined by estimating the covariance functions between the current speed and wave free-surface displacement for time lags from 0 - 10 seconds. Oscillations of the covariance function can indicate both the amplitude and phase of any gross response of the current meter to the wave perturbations. The relation is given by:

$$\phi_{un}(k\Delta t) = \frac{1}{T-k\Delta t} \sum_{t=o}^{T/\Delta t - k} u(i\Delta t)n(i\Delta t + k\Delta t), \qquad (7)$$

where k is the number of lags when k = 0,1,2, . . . 10. Δt is the sampling time interval = 1 second. T is the total length of the time series = 20 minutes (1200 seconds).

Figure 30 shows the normalized covariance functions for the three records appearing in figure 29. The 19 May record, associated with small wave heights, displays insignificant correlation irrespective of lags up to 10 seconds. The 21 May record displays some in-phase coupling at zero lag and a periodicity of 4-6 seconds, which corresponds to the waves themselves (figure 29). The 23 May record displays a relatively large amplitude oscillation that is initially of opposite phase or inverse that of record 21 May and has a period of 9-10 seconds.

Examination of more covariance functions reveals similar patterns of in-phase behavior for 6-12 hours then a shift to an out-of-phase relationship. The amplitude, as expected, does increase generally with the wave energy.

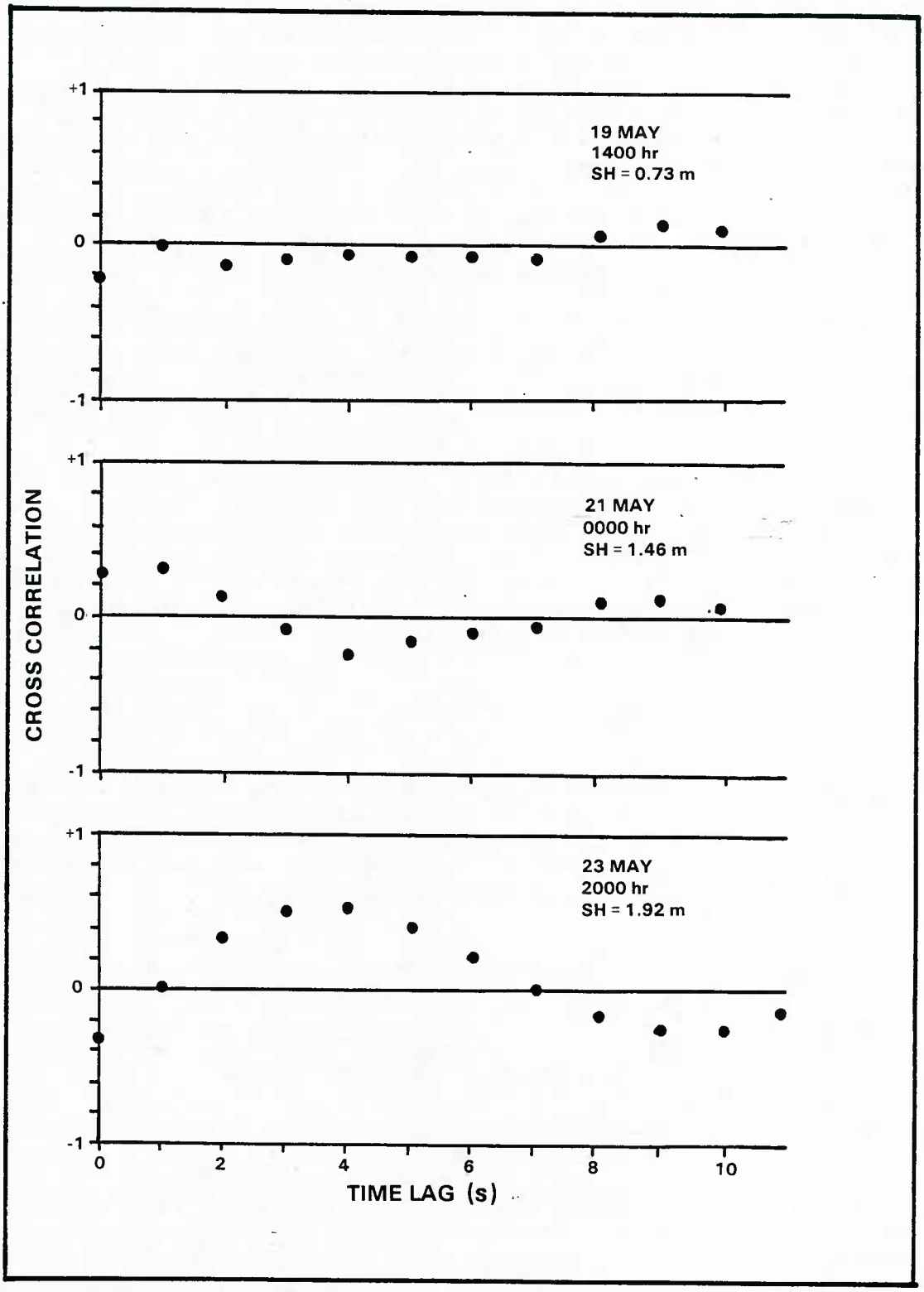

Figure 30. Normalized Covariance Function Estimated for the Record Pairs Shown in Figure 28 for Ten 1-Second Lags

From an examination of the response of the current speed signal and the covariances to the higher waves, it appears that a threshold occurs whereby the response or coupling of the current meter increases rapidly with increased wave heights. The oscillatory signal, i.e., in the 23 May record (figure 29) can of course be filtered out; however, it is possible that some low frequency energy could produce a rectification effect that would increase the mean current levels.

The covariance plots show that there is no obvious doubling of the wave frequency, i.e., no indication of the dominant effect of the mooring line perturbing the tether as suggested by equation (5).

These preliminary results suggest that for moderate sea conditions, i.e., significant wave heights up to 1.7 meters, little, if any, bias should occur in the current speeds monitored at 5 meters below the wave buoy. Higher sea conditions may require some filtering (and caution) in estimating mean current.

Further examination of the effects of wave motions on the ability to measure surface currents is required. Spectral analysis of both the wave heave and current records should be made. These records would indicate the threshold of the tether perturbations that would impart a frequency doubling of that of the surface waves. Also, the wave orbital motions interacting directly with the current meter could produce a variety of complex effects, many of which may not tend to "average out."

CONCLUSIONS

Weapon tests and evaluations made at undersea ranges or in the open ocean normally require a measure, or at least an indication, of sea state or wave conditions. It is widely recognized that higher energy wind and wave conditions have adverse effects upon the operation of both weapon systems and sonars; in fact, many systems or operations using them are so called "sea state limited."

In spite of the importance of this critical parameter, sea state is not directly measured by any reliable sensors or techniques. Furthermore, its very definition is not suitable to describe numerically the actual sea surface which is, in fact, a complex assemblage of both seas and swell of varying amplitudes and directions of propagation. Moreover, there is no standard measure or definition of white capping or surface turbulence intensity, factors which appear even more critical to near-surface acoustic performance than the sea surface roughness.

The development of the URI/ENDECO Type 956 directional wave-track buoy system represents a potential breakthrough in the difficult problem of surface wave measurement. The attributes of the new system rest principally on: (1) its ability to sense directivity of waves at a single point in the ocean, i.e., not requiring an elaborate cumbersome float array or series of individual sensors, (2) real-time transmission of the wave information, thus facilitating rapid data analysis with minicomputers, and (3) relative ease of deployment and recovery--not requiring a large vessel or heavy hoisting equipment.

The use of both the 956 and 1015 ENDECO systems during a NUSC-sponsored WEAP experiment south of Block Island, RI demonstrated both systems' usefulness and reliability in remotely measuring important sea and swell, and surface current parameters. These data were transmitted several kilometers to receiving stations and provided output in both real-time and nonreal-time modes. Similar use of these systems during future weapon testing and evaluation should be encouraged for the following reasons: (1) wave conditions of height and direction and near-surface currents will provide, in real time, quantitative environmental data never before available to weapons test operations; (2) since these data can also be conveniently recorded on magnetic disk, the data and related statistics can be used in post-test analysis to effectively assess how the sea surface environment adversely affects the performance of weapons. Clearly, such systems would vastly improve the capability for in situ evaluations of underwater weapons and sonars.

Tests of ENDECO 1015 system indicate that it is a useful tool for deployment in oil spill cleanup operations. The system can be readily assembled and checked out in 15-20 minutes. Deployment can be performed in small boats since the system utilizes lightweight, easy-to-handle ground tackle. This permits flexibility in geographic positioning retrieval, and redeployment to maintain observations in the vicinity of the spill undergoing gross horizontal advection. On the basis of the WEAP experiment, the ENDECO 1015 system appears quite suitable for providing real-time wave and current information critical to oil spill cleanup operations.

REFERENCES

1. Type 956 Directional Wave-Track Buoy System, Specification Data Sheet No. 79, ENDECO, Inc., Marion, MA, 1982.

2. R. Chapman and H. Scott, "Surface Backscattering Strengths Measured Over an Extended Range of Frequencies and Grazing Angles," Journal of the Acoustical Society of America, vol. 36, 1964, p. 1735.

3. H. W. Marsh, M. Schulkin, and S. Kneale, "Scattering of Underwater Sound by the Sea Surface," Journal of the Acoustical Society of America, vol. 33, 1961, p. 334.

4. M. Schulkin and R. Shaffer, "Backscattering of Sound From the Sea Surface," Journal of the Acoustical Society of America, vol. 36, 1964 p. 1699.

5. C. S. Clay and H. Medwin, Acoustical Oceanography: Principles and Applications, John Wiley & Sons, Inc., NY, 1977.

6. F. Middleton, L. R. LeBlanc, and W. I. Sternberger, "Wave Direction Measurement by a Single Wave Follower Buoy," Proceedings of the 10th Annual Offshore Technology Conference, Houston, TX, 1978.

7. ENDECO Type 956 Directional Wave-Track Buoy System Program Documentation, ENDECO, Inc., Marion, MA, 1981.

8. E. O. Brigham, The Fast Fourier Transform, Prentice-Hall, Inc., Englewood Cliffs, NJ, 1984, 253 p.

9. L. LeBlanc and F. Middleton, "Storm Directional Wave Spectra Measured with a Single Buoy," Oceans 82, Proceedings of the Institute of Electrical and Electronic Engineers, 1982.

10. N. F. Barber, Measurements of Sea Conditions by Motion of a Floating Buoy, A.R.L./103.40/N/22/W, Admiralty Research Laboratory, Teddington, Middlesex, England, 1946.

11. M. Longuet-Higgins, D. Cartwright, and N. Smith, "Observations of the Directional Spectrum of Sea Waves Using the Motions of a Floating Buoy," Ocean Wave Spectra, U.S. Naval Oceanographic Office and National Academy of Sciences, Prentice-Hall, Inc., Englewood Cliffs, NJ, 1963.

12. D. H. Shonting, "Rhode Island Sound Square Kilometer Study 1967: Flow Patterns and Kinetic Energy Distribution," Journal of Geophysics Research, vol. 74, no. 13, 1969, pp. 3386-3395.

13. M. Triantafyllou and R. Salter, "The Design of the Mooring System for a Tethered Current Meter," Ph.D. Dissertation, Massachusetts Institute of Technology, 1980.

14. DTNSRDC Calibration Data prepared for ENDECO, Marion, MA, 1976.

APPENDIX A

DETAILS OF WAVE DATA PROCESSING

DATA TRANSMISSION

The ENDECO Type 956 directional wave-track buoy registered wave heave (free surface elevation) on channel 1, east-west tilt on channel 2, and north-south tilt on channel 3. The ENDECO Type 1015 wave-track/current meter buoy registered wave heave on channel 1, current speed on channel 2, and current direction (magnetic) on channel 3.

Prior to buoy deployment each FM transmitter was programmed so that data were transmitted from the 956 system at the beginning of every odd hour and from the 1015 buoy every even hour. Each transmission was continuous for 20 minutes. Thus a 20-minute record was available from a particular buoy every 2 hours, whereas a free surface (heave) record was obtained each hour.

Data were received and processed aboard the USNS LYNCH and at the Block Island Field Station at Monhegan Bluffs as indicated in figure 8.

DATA COLLECTION AND PROCESSING ABOARD THE USNS LYNCH

The received FM signals for each of the three channels from each buoy were converted to 8-bit digital values by the ENDECO 956 receiver which provided sampling intervals of 1.0 or 0.5 second. The processing sequence is described in the following paragraphs.

Recording Data with the Memodyne M-80

The receiver generated a value for each of the three channels once every second or half second during the 20-minute sampling interval. A Memodyne M-80 microprocessor transferred the values, formatted in 8-bit words from the receiver to cassettes for primary storage. On cassettes, values were recorded serially in the order they were received, i.e., channels 1,2,3,1,2,3, etc. Time and frame marks (for data alignment into proper channels) inserted into the data stream by the receiver were also recorded. Buffer size within the M-80 was 256 bytes; data were quite densely packed by minimizing the number of interblock gaps. While no data were being sent from the receiver, the M-80 recorder awaited receiver input.

Backup of Data from M-80 to Hewlett Packard (HP) Diskettes

Data were stored off-line on HP diskettes via the onboard, 9825A mini-computer. (A diskette has 2.3 times the byte storage of the HP cassette.) Data recording was suspended during tape backup onto disk. An HP 16-bit interface unit, configured to match the M-80 default mode at 110 baud (bits per second), connected the HP with the M-80, via an adapter plug, which jumpered pins 4 and 5 ("request to send" and "clear to send") on the M-80 side.

The "binary-write" mode of the M-80 during data recording precluded reception of command through its serial port; all input was interpreted as binary data to prevent disruption of recording by reception of a bit sequence that coincided with a command code. A "system reset" of the unit was performed on the unit via front panel controls to enable control of the recorder by the HP computer. Unfortunately, the system reset also purged the 256-byte data buffer, which may have contained up to 255 bytes of unrecorded data. Because of this purge and because both the 956 receiver and the HP computer used the same RS-232 port on the rear panel of the M-80, data collection was precluded during disk backup.

The program named M-80BEN (and later M80CEN) transferred the data block-by-block from the M-80 to HP disks without interpretation. Once transferred to HP disk, the data could be analyzed on the HP system exclusively, freeing the M-80 unit for collection of new data.

Analysis of Data Stored on HP Disk

The program PLOTR produced three time series plots describing the input of the three channels for each 20-minute data segment on the HP 9872A flatbed plotter. Using hour marks inserted into the data stream by the 956 receiver, the program searched an entire disk for any requested 20-minute segment of data. Proper titles and labels were chosen according to the incremental hour marker parity; data from different buoys were thereby differentiated. PLOTR used "frame marks," consisting of a triplet of zeros that replaced every 128th triplet of data values, to sort the data into proper channels; errors introduced by accidental loss of data were thus minimized.

Setup of the M-80 Recorder by the HP System

The M-80 was programmed through the serial interface. Two HP system programs set up the M-80 recorder for data collection:

1) VIRGN; (a) Filled the entire tape with one large interblock gap (erase), (b) rewound and advanced the tape to the load point, (c) put the M-80 in "binary-write" mode.

2) STRC2; (a) Advanced tape to a point beyond the last previously written block of data, (b) placed the M-80 in "binary-write" mode. This program enabled reuse of a tape cassette without destruction of previously recorded data.

Data Analysis

Preliminary data analysis made at NUSC after the WEAP cruise consisted of plotting and estimating correlation coefficients between wave free-surface elevation and current speed and direction. Preparation was made to enable transfer of the entire data set of the Type 956 directional wave-track system from the HP diskettes into a VAX 11/780 computer for further spectral analysis.

APPENDIX B

SAMPLES OF TARBELL ESTIMATES OF WAVE STATISTICS FOR VARIOUS WAVE CONDITIONS (STATISTICS ARE BASED UPON WAVE HEIGHTS IN FEET)

1- 19/MAY/83
$21^h:01^m$

1054 POINTS READ IN.

HEAVE

MEAN	STDV	SPIKES	RAW MAX	RAW MIN	FIN MAX	FIN MIN
131.7	1.20	1	159.	64.	5.33	-3.26

N-S TILT

MEAN	STDV	SPIKES	RAW MAX	RAW MIN	FIN MAX	FIN MIN
131.1	6.45	0	212.	87.	28.43	-15.51

E-W TILT

MEAN	STDV	SPIKES	RAW MAX	RAW MIN	FIN MAX	FIN MIN
126.6	5.79	1	246.	86.	24.39	-14.28

1054 GOOD DATA POINTS IN EACH SERIES. SEGMENT LENGTH = 1024

REVISED MAXIMA/MINIMA
HEAVE
MAXIMUM READING: 4.75 MINIMUM READING: -3.26
N-S TILT
MAXIMUM READING: 28.43 MINIMUM READING:-15.51
E-W TILT
MAXIMUM READING: 24.39 MINIMUM READING:-14.28

STATISTICS
START: 5/19/82 -- 21: 1:14

NBR WAVES:	212	PERIOD OF MAX HEIGHT:	21.0
MAX PERIOD:	21.0	SIGNIFICANT PERIOD:	5.2
MEAN PERIOD:	4.8	SIGNIFICANT HEIGHT:	4.0
MEAN HEIGHT:	2.6	HEIGHT VARIANCE:	1.4
MAX HEIGHT:	6.1	ROOT-MEAN-SQ HEIGHT:	2.9

PROFILE OF MAXIMUM WAVE AT 1.00 SECOND INTERVALS

-2.7	1.1	2.4	.3	.8	1.9	3.4	1.3	.6	3.0	1.4	2.1
.4	1.6	2.4	1.0	.6	.3	.4	.3	-.5	-1.3	.4	

FREQUENCY BANDNUMBER	CENTER FREQUENCY	CENTER PERIOD	ENERGY DENSITY	MEAN DIRECTION	STANDARD DEVIATION
1	.038	26.6	12.28	6.	13.1
2	.047	21.3	4.29	4.	13.2
3	.060	16.8	1.43	7.	8.7
4	.075	13.3	.28	4.	10.2
5	.097	10.3	1.07	23.	19.9
6	.127	7.9	.85	285.	31.7
7	.171	5.8	2.54	228.	16.5
8	.225	4.5	10.68	226.	13.8
9	.292	3.4	3.11	314.	24.0
10	.417	2.4	.90	350.	28.2

ENVIRONMENTAL DEVICES CORPORATION
DIRECTIONAL WAVE BUOY DATA PROCESSING - 1017
VERSION 1.4 - 1/82

WAITING FOR DATA.

2- 19/MAY/83
08h:01m

1054 POINTS READ IN.

HEAVE

MEAN	STDV	SPIKES	RAW MAX	RAW MIN	FIN MAX	FIN MIN
136.9	.68	1	153.	55.	3.15	-1.54

N-S TILT

MEAN	STDV	SPIKES	RAW MAX	RAW MIN	FIN MAX	FIN MIN
17.4	1.69	0	123.	13.	1.63	-1.53

E-W TILT

MEAN	STDV	SPIKES	RAW MAX	RAW MIN	FIN MAX	FIN MIN
15.1	5.85	0	112.	2.	14.01	-4.62

1052 GOOD DATA POINTS IN EACH SERIES. SEGMENT LENGTH = 1024

REVISED MAXIMA/MINIMA
HEAVE
MAXIMUM READING: 1.78 MINIMUM READING: -1.54
N-S TILT
MAXIMUM READING: 1.63 MINIMUM READING: -1.53
E-W TILT
MAXIMUM READING: 14.01 MINIMUM READING: -4.62

STATISTICS
START: 5/19/82 -- 8: 1:14

NBR WAVES:	224	PERIOD OF MAX HEIGHT:	6.0
MAX PERIOD:	10.0	SIGNIFICANT PERIOD:	5.5
MEAN PERIOD:	4.5	SIGNIFICANT HEIGHT:	1.6
MEAN HEIGHT:	1.1	HEIGHT VARIANCE:	.2
MAX HEIGHT:	2.9	ROOT-MEAN-SQ HEIGHT:	1.2

PROFILE OF MAXIMUM WAVE AT 1.00 SECOND INTERVALS

-1.0	.3	2.0	.3	,3	.2	-.3	.4

FREQUENCY BANDNUMBER	CENTER FREQUENCY	CENTER PERIOD	ENERGY DENSITY	MEAN DIRECTION	STANDARD DEVIATION
1	.038	26.6	.24	38.	12.7
2	.047	21.3	.11	54.	22.1
3	.060	16.8	.06	57.	28.9
4	.075	13.3	.16	47.	41.4
5	.097	10.3	1.06	66.	15.7
6	.127	7.9	.89	87.	34.0
7	.171	5.8	.45	53.	26.2
8	.225	4.5	.66	63.	16.5
9	.292	3.4	.76	81.	35.8
10	.417	2.4	.24	70.	21.0

ENVIRONMENTAL DEVICES CORPORATION
DIRECTIONAL WAVE BUOY DATA PROCESSING - 1017
VERSION 1.4 - 1/82

WAITING FOR DATA.

3- 20/MAY/83
19h:04m

. 798 POINTS READ IN.

WAVE
MEAN	STDV	SPIKES	RAW MAX	RAW MIN	FIN MAX	FIN MIN
131.3	1.71	1	163.	60.	6.30	-4.93

N-S TILT
MEAN	STDV	SPIKES	RAW MAX	RAW MIN	FIN MAX	FIN MIN
121.1	4.90	0	168.	79.	16.49	-14.79

E-W TILT
MEAN	STDV	SPIKES	RAW MAX	RAW MIN	FIN MAX	FIN MIN
120.5	4.72	0	187.	77.	23.39	-15.29

798 GOOD DATA POINTS IN EACH SERIES. SEGMENT LENGTH = 512

REVISED MAXIMA/MINIMA
WAVE
MAXIMUM READING: 5.81 MINIMUM READING: -3.96
N-S TILT
MAXIMUM READING: 16.49 MINIMUM READING:-14.79
E-W TILT
MAXIMUM READING: 23.39 MINIMUM READING:-15.29

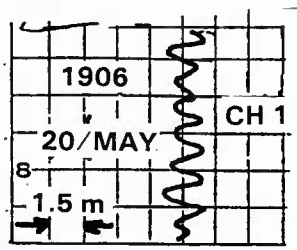

RUSTRAC RECORD

STATISTICS
START: 5/20/82 -- 19: 4:40

NR WAVES:	90	PERIOD OF MAX HEIGHT:	8.0
MA PERIOD:	11.0	SIGNIFICANT PERIOD:	6.5
MEAN PERIOD:	5.7	SIGNIFICANT HEIGHT:	5.9
MEAN HEIGHT:	3.8	HEIGHT VARIANCE:	3.6
MAX HEIGHT:	8.8	ROOT-MEAN-SQ HEIGHT:	4.2

PROFILE OF MAXIMUM WAVE AT 1.00 SECOND INTERVALS

-.0	.5	1.1	1.7	3.2	-1.2	-4.7	-5.6	-1.1	2.5

FREQUENCY BANDNUMBER	CENTER FREQUENCY	CENTER PERIOD	ENERGY DENSITY	MEAN DIRECTION	STANDARD DEVIATION
1	.038	26.3	5.76	352.	7.1
2	.047	21.3	4.29	56.	40.0
3	.060	16.8	.75	335.	26.2
4	.075	13.3	.64	213.	25.9
5	.097	10.3	3.36	295.	23.8
6	.127	7.9	27.10	185.	19.8
7	.172	5.8	14.61	194.	13.7
8	.225	4.5	6.79	228.	15.5
9	.291	3.4	1.93	300.	31.7
10	.416	2.4	.79	113.	24.1

ENVIRONMENTAL DEVICES CORPORATION
DIRECTIONAL WAVE BUOY DATA PROCESSING - 1017
VERSION 1.4 - 1/82

4- 23/MAY/82
17h:01m 14s

1054 POINTS READ IN.

HEAVE

MEAN	STDV	SPIKES	RAW MAX	RAW MIN	FIN MAX	FIN MIN
131.8	1.67	1	157.	56.	4.93	-4.64

N-S TILT

MEAN	STDV	SPIKES	RAW MAX	RAW MIN	FIN MAX	FIN MIN
117.3	5.97	0	166.	47.	17.13	-24.70

E-W TILT

MEAN	STDV	SPIKES	RAW MAX	RAW MIN	FIN MAX	FIN MIN
113.8	7.05	0	164.	16.	17.64	-34.39

1054 GOOD DATA POINTS IN EACH SERIES. SEGMENT LENGTH = 1024

REVISED MAXIMA/MINIMA
HEAVE
MAXIMUM READING: 4.93 MINIMUM READING: -4.64
N-S TILT
MAXIMUM READING: 17.13 MINIMUM READING:-24.70
E-W TILT
MAXIMUM READING: 17.64 MINIMUM READING:-34.39

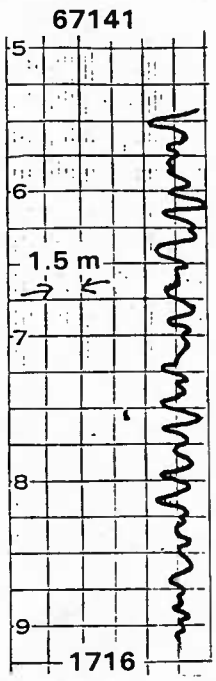

STATISTICS
START: 5/23/82 -- 17: 1:14

NBR WAVES:	193	PERIOD OF MAX HEIGHT:	6.0
MAX PERIOD:	14.0	SIGNIFICANT PERIOD:	6.5
MEAN PERIOD:	5.3	SIGNIFICANT HEIGHT:	5.8
MEAN HEIGHT:	3.8	HEIGHT VARIANCE:	3.1
MAX HEIGHT:	8.6	ROOT-MEAN-SQ HEIGHT:	4.2

PROFILE OF MAXIMUM WAVE AT 1.00 SECOND INTERVALS

-4.0	.5	2.5	4.6	2.4	-1.8	-1.9	1.7

FREQUENCY BANDNUMBER	CENTER FREQUENCY	CENTER PERIOD	ENERGY DENSITY	MEAN DIRECTION	STANDARD DEVIATION
1	.038	26.6	12.19	186.	24.4
2	.047	21.3	7.81	211.	18.1
3	.060	16.8	2.37	225.	10.7
4	.075	13.3	1.28	217.	12.3
5	.097	10.3	4.21	0.	17.0
6	.127	7.9	12.11	142.	21.0
7	.171	5.8	13.90	122.	15.5
8	.225	4.5	9.89	118.	13.0
9	.292	3.4	4.87	63.	21.6
10	.417	2.4	1.24	307.	24.5

ENVIRONMENTAL DEVICES CORPORATION
DIRECTIONAL WAVE BUOY DATA PROCESSING - 1017
VERSION 1.4 - 1/82

5- 23/MAY/82
19h:01m

1054 POINTS READ IN.

HEAVE

MEAN	STDV	SPIKES	RAW MAX	RAW MIN	FIN MAX	FIN MIN
131.9	1.89	1	165.	78.	6.47	-5.64

N-S TILT

MEAN	STDV	SPIKES	RAW MAX	RAW MIN	FIN MAX	FIN MIN
113.9	6.29	1	190.	0.	26.77	-27.02

E-W TILT

MEAN	STDV	SPIKES	RAW MAX	RAW MIN	FIN MAX	FIN MIN
121.7	7.18	0	169.	22.	16.63	-35.05

1054 GOOD DATA POINTS IN EACH SERIES. SEGMENT LENGTH = 1024

REVISED MAXIMA/MINIMA
HEAVE
MAXIMUM READING: 6.47 MINIMUM READING: -5.64
N-S TILT
MAXIMUM READING: 26.77 MINIMUM READING:-27.02
E-W TILT
MAXIMUM READING: 16.63 MINIMUM READING:-35.05

STATISTICS
START: 5/23/82 -- 19: 1:14

NBR WAVES:	170	PERIOD OF MAX HEIGHT:	10.0
MAX PERIOD:	18.0	SIGNIFICANT PERIOD:	7.6
MEAN PERIOD:	6.0	SIGNIFICANT HEIGHT:	6.8
MEAN HEIGHT:	4.6	HEIGHT VARIANCE:	3.8
MAX HEIGHT:	9.6	ROOT-MEAN-SQ HEIGHT:	5.0

PROFILE OF MAXIMUM WAVE AT 1.00 SECOND INTERVALS

-.4	3.2	1.8	.8	1.5	2.0	1.9	-1.8	-4.9	-6.4	-.9	1.4

FREQUENCY BANDNUMBER	CENTER FREQUENCY	CENTER PERIOD	ENERGY DENSITY	MEAN DIRECTION	STANDARD DEVIATION
1	.038	26.6	36.20	285.	23.4
2	.047	21.3	13.34	284.	26.3
3	.060	16.8	3.71	262.	14.8
4	.075	13.3	.69	301.	29.9
5	.097	10.3	3.79	101.	23.9
6	.127	7.9	24.24	145.	13.0
7	.171	5.8	15.12	112.	13.3
8	.225	4.5	11.75	93.	19.2
9	.292	3.4	4.94	51.	24.0
10	.417	2.4	1.23	326.	24.9

ENVIRONMENTAL DEVICES CORPORATION
DIRECTIONAL WAVE BUOY DATA PROCESSING - 1017
VERSION 1.4 - 1/82

WAITING FOR DATA.

6- 24/MAY/82
15h:01m

1054 POINTS READ IN.

HEAVE

MEAN	STDV	SPIKES	RAW MAX	RAW MIN	FIN MAX	FIN MIN
131.6	1.12	0	152.	116.	3.98	-3.05

N-S TILT

MEAN	STDV	SPIKES	RAW MAX	RAW MIN	FIN MAX	FIN MIN
121.0	3.95	0	157.	73.	12.65	-16.89

E-W TILT

MEAN	STDV	SPIKES	RAW MAX	RAW MIN	FIN MAX	FIN MIN
122.7	4.32	2	158.	86.	12.40	-18.54

1054 GOOD DATA POINTS IN EACH SERIES. SEGMENT LENGTH = 1024

REVISED MAXIMA/MINIMA
HEAVE
MAXIMUM READING: 3.98 MINIMUM READING: -3.05
N-S TILT
MAXIMUM READING: 11.94 MINIMUM READING:-16.89
E-W TILT
MAXIMUM READING: 12.40 MINIMUM READING:-18.54

STATISTICS
START: 5/24/82 -- 15: 1:14

NBR WAVES:	171	PERIOD OF MAX HEIGHT:	9.0
MAX PERIOD:	12.0	SIGNIFICANT PERIOD:	7.5
MEAN PERIOD:	5.9	SIGNIFICANT HEIGHT:	4.3
MEAN HEIGHT:	2.7	HEIGHT VARIANCE:	1.7
MAX HEIGHT:	6.0	ROOT-MEAN-SQ HEIGHT:	3.0

PROFILE OF MAXIMUM WAVE AT 1.00 SECOND INTERVALS

-2.4	.3	1.9	2.8	1.7	-.2	-1.9	-3.0	-3.2	-.3	1.1

FREQUENCY BANDNUMBER	CENTER FREQUENCY	CENTER PERIOD	ENERGY DENSITY	MEAN DIRECTION	STANDARD DEVIATION
1	.038	26.6	.78	358.	11.0
2	.047	21.3	.70	328.	44.4
3	.060	16.8	.52	349.	19.4
4	.075	13.3	.29	358.	8.3
5	.097	10.3	9.75	18.	27.1
6	.127	7.9	14.61	146.	18.4
7	.171	5.8	4.24	112.	11.2
8	.225	4.5	1.83	116.	13.6
9	.292	3.4	1.17	352.	21.7
10	.417	2.4	.67	286.	23.6

ENVIRONMENTAL DEVICES CORPORATION
DIRECTIONAL WAVE BUOY DATA PROCESSING - 1017
VERSION 1.4 - 1/82

WAITING FOR DATA

1054 POINTS READ IN.

HEAVE

MEAN	STDV	SPIKES	RAW MAX	RAW MIN	FIN MAX	FIN MIN
151.9	1.02	1	153.	73.	4.13	-2.71

N-S TILT

MEAN	STDV	SPIKES	RAW MAX	RAW MIN	FIN MAX	FIN MIN
129.2	1.74	1	155.	114.	5.54	-5.36

E-W TILT

MEAN	STDV	SPIKES	RAW MAX	RAW MIN	FIN MAX	FIN MIN
125.9	2.12	0	156.	105.	10.57	-7.36

1054 GOOD DATA POINTS IN EACH SERIES. SEGMENT LENGTH = 1024

REVISED MAXIMA/MINIMA
HEAVE
MAXIMUM READING: 3.15 MINIMUM READING: -2.71
N-S TILT
MAXIMUM READING: 5.54 MINIMUM READING: -5.36
E-W TILT
MAXIMUM READING: 5.65 MINIMUM READING: -7.36

STATISTICS
START: 5/25/82 -- 3: 1:14

NBR WAVES:	137	PERIOD OF MAX HEIGHT:	7.0
MAX PERIOD:	12.0	SIGNIFICANT PERIOD:	8.6
MEAN PERIOD:	7.4	SIGNIFICANT HEIGHT:	3.7
MEAN HEIGHT:	2.5	HEIGHT VARIANCE:	1.2
MAX HEIGHT:	5.8	ROOT-MEAN-SQ HEIGHT:	2.7

PROFILE OF MAXIMUM WAVE AT 1.00 SECOND INTERVALS

-1.2	.2	1.6	2.4	.6	-2.2	-3.4	-2.2	.9

FREQUENCY BANDNUMBER	CENTER FREQUENCY	CENTER PERIOD	ENERGY DENSITY	MEAN DIRECTION	STANDARD DEVIATION
1	.038	26.6	.38	349.	33.2
2	.047	21.3	.27	267.	41.5
3	.060	16.8	.18	63.	31.2
4	.075	13.3	.50	27.	19.4
5	.097	10.3	9.89	141.	13.6
6	.127	7.9	11.93	139.	7.1
7	.171	5.8	3.13	134.	10.0
8	.225	4.5	.78	126.	8.8
9	.292	3.4	.26	93.	21.2
10	.417	2.4	.12	249.	24.2

ENVIRONMENTAL DEVICES CORPORATION
DIRECTIONAL WAVE BUOY DATA PROCESSING - 1017
VERSION 1.4 - 1/82

WAITING FOR DATA.

INITIAL DISTRIBUTION LIST

Addressee	No. of Copies
CNR (ONR-480, ONR-481--2 copies, ONR-483, ONR-485--2 copies)	6
COMNAVSEASYSCOM (SEA-003, SEA-03)	2
COMNAVOCEANCOM, Bay St. Louis	1
NRL, Bay St. Louis	1
NRL/USRD, Orlando	1
NORDA, Bay St. Louis (Code 110--R. Goodman)	1
NAVOCEANO, Bay St. Louis	1
NOSC, San Diego (Attn: Technical Library)	1
NPS, Monterey	1
NWC, Newport	1
NETC, Newport	1
APL, Univ. of Washington	1
ARL, Penn State	1
ARL, Univ. of Texas	1
Marine Physical Laboratory, Scripps	1
NOAA/ERL, Boulder	1
WHOI, Woods Hole	1
DTIC, Alexandria	2
U.S. Geological Survey, Water Resources Div., Reston	1
Automation Industries, Vitro Labs (Attn: D.J. O'Neill)	1